Fall 2014

Data analysis and summary for surfactant-polymer flooding based on oil field projects and laboratory data

Pratap D. Chauhan

Department:

DATA ANALYSIS AND SUMMARY FOR SURFACTANT-POLYMER FLOODING BASED ON OIL FIELD PROJECTS AND LABORATORY DATA

by

PRATAP D. CHAUHAN

A THESIS

Presented to the Faculty of the Graduate School of the

MISSOURI UNIVERSITY OF SCIENCE AND TECHNOLOGY

In Partial Fulfillment of the Requirements for the Degree

MASTER OF SCIENCE IN PETROLEUM ENGINEERING

2014

Approved by

Dr. Baojun Bai, Advisor
Dr. Mingzhen Wei
Dr. Ralph Flori

ABSTRACT

Enhanced oil recovery screening is considered as an important first step towards evaluating a potential EOR technique for a candidate reservoir. A vast amount of research is continuously been conducted in EOR. Therefore, it is imperative to update the screening criteria regularly.

This study involves updating the screening criteria for surfactant polymer flooding for field projects dataset and laboratory dataset. Many of the screening criteria for surfactant-polymer flooding in the literature were achieved on the basis of data collected from the EOR surveys published biennially in Oil & Gas Journals. However, these datasets contain problems like missing data and inconsistent data. Data quality has not been addressed in the previous works in the literature on screening criteria. The objective of this study was to update achieve a range for 42 surfactant-polymer projects after the data. Another comprehensive work of this study was to establish a range for laboratory dataset consisting of 200 experiments.

Box-plots and Cross-plots were used to study the dataset for special cases or inconsistent data. Histograms and box-plots were used to exhibit the distribution of each parameter and present the range of the dataset.

Eventually, the ranges for field projects were compared with the screening criteria previously published in the literature. Also, the developed screening criteria for laboratory work were compared with the developed screening criteria for oilfield projects.

ACKNOWLEDGMENTS

This thesis would not have been possible without the help and constant support of my advisor Dr. Baojun Bai. I thank him for accepting me as one of his graduate student and constantly guiding me, with utmost patience to become a better engineer.

I am also thankful to my research committee members Dr. Mingzhen Wei and Dr. Ralph Flori for providing their timely guidance.

I would also like to mention my sincere thanks to my friends in US, especially, Ronak V. Shah, Poda, Laxmikanth and Paul, as well as friends back home for constantly motivating me to publish this work.

And last but not the least, I would like to sincerely acknowledge my mother and grandmother, without whose blessings pursuing an engineering degree would not have been possible.

TABLE OF CONTENTS

Page

LIST OF ILLUSTRATIONS

Page

LIST OF TABLES

Page

1. INTRODUCTION

Oil recovery processes have been traditionally classified as Primary, Secondary and Tertiary. This classification of oil recovery methods is not necessarily chronological, for instance a reservoir having heavy oil will be deemed unworthy for primary recovery and waterflooding, hence tertiary methods (EOR) would be used for extraction (Paul Willhite et al., 1998). This makes the classification dubious. However, the words Tertiary Oil Recovery and Enhanced Oil Recovery (also referred here in as 'EOR') have been used interchangeably.

The 19th century witnessed discoveries of major oilfields in regions such as the Slope of Alaska, the North Sea, Indonesia, the South American continent and needless to say the Middle East. However, all the major oil reservoirs have started to witness a decline in production and increase in water-cut (Avg. water-cut increased from 75% to 80% between 1999-2004) and oil companies have been compelled to think out of their comfort zone, which has given rise to unconventional oil recovery methods. EOR methods fall under the category of these Unconventional methods. The scope of EOR methods is emphasized when nearly 2/3rd of the oil in the reservoir is left un-extracted after primary and secondary methods. US, alone has a massive 351 billion barrels out of a 536 billion barrels (OOIP) of oil which remains trapped in the reservoir rock after the conventional methods have been applied. Moreover, Gulf of Mexico has a whopping 40 billion barrels of remaining oil in place. These facts shed some light on the promising future that lies ahead for various EOR methods. Hence, there has been a vast amount of

research, both in Field and in Laboratory being carried out to improve the efficiency of EOR methods. The research in EOR spiked up impressively in 1980's as the oil prices increased exponentially. However, since then most of the EOR methods are sparsely used as the oil price kept fluctuating. Although, the recent stability in oil prices has initiated a good amount of research which would help fill the technology gaps that hamper the efficiency with which the EOR methods are applied. This suggests that the frequency with which EOR methods are applied depends majorly on the oil price. Also, for a successful EOR operation, it is imperative that the overall cost of the operation does not exceed the cost of the total oil extracted with its help. Hence, evaluation of the EOR methods remains a key factor in their success.

This study is an attempt to evaluate one of the EOR methods called as Surfactant-Polymer Flooding. It aims at evaluation of Surfactants and to infer a suitable Screening Criteria for the same.

2. LITERATURE REVIEW

2.1 EOR- CONCEPT AND TYPES

2.1.1. Concept. Paul and Willhite (1998) describe EOR as the process of injecting one or more than one fluids which are not present in the reservoir to increase the production of residual oil or remaining oil after primary and secondary recovery. These injected fluids sometimes also assist the primary energy in the reservoir. The injected fluids interact with the rock-oil system physically or chemically to maximize the recovery of oil.

IOR (Improved Oil Recovery) is often mistaken to be a term identical to EOR. Although, IOR includes all the processes which come under EOR, it is more of a holistic term which includes all the other methods which improve the recovery of oil in any way. Hence, IOR will also encompass processes such as Hydraulic Fracturing or Infill Drilling to name a few.

2.1.2. EOR Classification and Description. EOR methods are classified into five different categories as mentioned below mobility-control, miscible, chemical, thermal and other processes (MEOR).

Mobility-control: Increase Volumetric Sweep Efficiency by achieving favorable mobility-ratio of the oil-water system and decreasing relative permeability of water. This is achieved by increasing the viscosity of water by adding viscous polymer to it or by

reducing mobility of gas by foam flooding to avoid viscous fingering. Can improve sweep efficiency of Surfactant flooding system.

Miscible: Includes injection of any material which mixes with the reservoir oil to form a fluid which flows with ease to the wells due to the improved mobility of the system. The first-contact-miscible (FCM) process acquires miscibility at the first contact with oil. Modification in the system is achieved when the injected phase acquires miscibility from multiple contacts with the oil (MCM). It is generally gases like CO_2 which are injected that result in reduction of the viscosity of oil after miscibility is achieved.

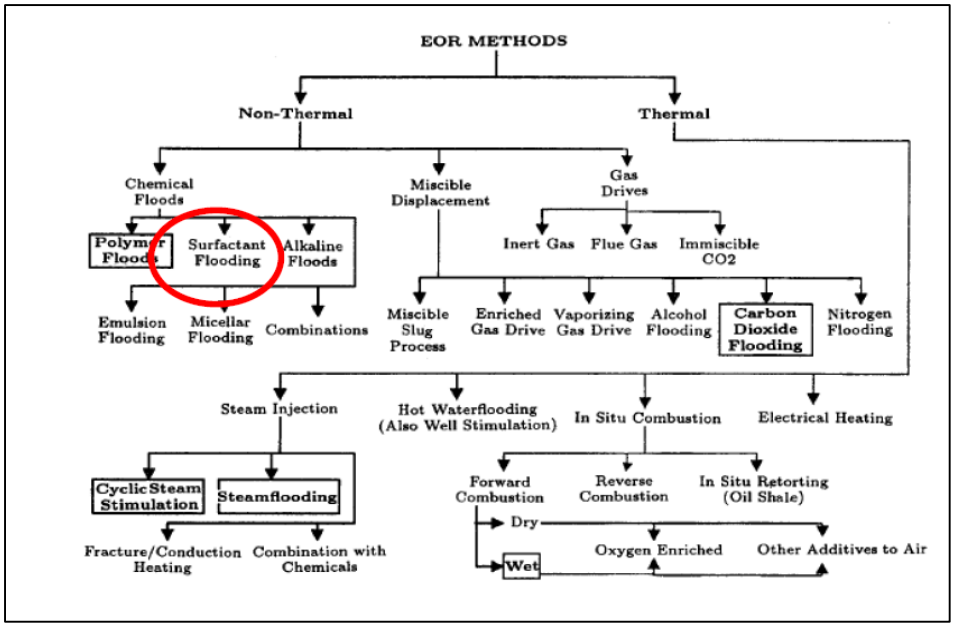

Figure 2.1 Types of EOR Methods (NTNU 2009)

Thermal: Includes injection of materials like steam, hot water or combustible gas (In-situ combustion). Thermal EOR processes use thermal energy to increase the recovery of oil. The oil's viscosity is reduced by the increase in temperature due to thermal energy. Steam methods are generally classified as cyclic steam simulation and steam drive. In-situ combustion involves burning a certain volume of gas to generate heat which vaporizing lighter parts of oil and reduction in oil viscosity.

MEOR: Microbes ferment hydrocarbons and produce by-products that are useful in the recovery of oil. MEOR uses the mechanism of channeling oil through preferred pathway in the reservoir by plugging off small channels so that oil is forced to migrate through larger pore spaces. Nutrients like sugar, phosphates or nitrates are injected to stimulate growth of microbes and aid their performance. The microbes generate surfactants and carbon dioxide that help to displace oil.

Chemical: Includes injection of chemicals which create desirable phase-behavior changes and there-by increase the recovery of oil. Although, polymer invariably increases the sweep-efficiency, the main mechanism by which recovery is achieved is decreasing the IFT between the displacing fluid and oil forcing the system to flow.

2.2 EOR CURRENT STATUS & FUTURE OPPORTUNITIES

A considerable portion of current world oil production comes from mature fields and the rate at which mature fields are replaced by newly discovered fields is negligible. To meet the ever increasing demand of oil throughout the world, the unconventionally recoverable oil left behind in the discovered reservoirs produced economically by EOR methods will be a challenge and play a key role in shaping the oil industry in future.

EOR methods have experienced an increasing interest, albeit the declining oil prices since 2008. The use of Thermal and Gas methods has been on a constant rise, as seen in Canada. Chemical methods have shown a constant decline in field application since 1980's. However, there have been a conclusive amount of pilot projects and laboratory research to keep the interest in chemical methods intact. China has seen the highest number of chemical projects carried out while France, US and India have also seen a few projects.

2.3 CHEMICAL EOR

Chemical EOR include tertiary techniques, which are based on application of chemical compounds and chemical processes relevant to the part of displacement mechanism of the reservoir oil. The mechanisms of chemical flooding include IFT reduction, wettability alteration, and mobility control.

Although, it is predicted that the world oil demand will nose dive from 60% (present) to 15% (2100), the fact remains that in all 250-260 billion tons of oil will be used to meet the world demand in years to come (University of Miskolc).

Chemical floods are basically classified into 3 types namely, polymers, surfactants and alkaline. The methods such as alkaline surfactant polymer flooding (ASP), Low tension water flooding (LTWF) and surfactant imbibition in carbonate reservoirs have been developed by the courtesy of research being carried out since the stroke of 21st century. The research has increased exponentially over the years due to diminishing conventional reserves, advances in technology and better understanding of failed projects. In the past and current century China has emerged as the leading country in the application of chemical EOR methods. Although, the USA has seen a fairly decent

amount of chemical EOR projects in different oil producing states of the country. The following figures below show the history of different chemical projects in the US and shows the total oil production due to chemical methods in China respectively.

Although, the application of chemical methods on large scale is not been advocated by the oil companies, a vast amount of research is being conducted to continuously to improve these methods. An imperative part of this research is being dedicated to the improvement of the recovery efficiency of such methods. New methods like surfactant imbibition, ASP are still at the nascent stage. Foam flooding is another chemical method which has emerged recently. However, research also needs to be carried out in using low concentrations of chemicals. Low concentration utilization will help the economics by reducing the cost of chemicals from the outset.

Energy Research and Development Administration (ERDA) now known as Department of Energy (DOE), have provided a vast amount of funding for chemical methods. The following table shows the amount of funding attributed towards chemical flooding methods (1974-1993).

Table 2.1 Summary of funding for Chemical Flooding projects (1974-1993)

Type	Number	Funding (USD)
Alkaline	4	5,493,403
Surfactant	3	65,005,101
Polymer	18	13,116,283
Total	75	85,828,787

2.4 SURFACTANT

The word surfactant stands for the portmanteau of the words ‘Surface’ and ‘Active’. Surfactants are amphiphilic in nature. It has an affinity to a polar medium (water) and a non-polar medium (hydrocarbon). The dual affinity of surfactant molecules result in a mono-layer between two mediums (Schramm. et. al., 2003). This mono-layer causes a decrease in interfacial tension (IFT) and forms a micro-emulsion between oil and water, this micro-emulsion, with low IFT moves with ease thorough the pore space.

The surfactant molecule consists of a hydrophilic head and a hydrophobic tail (Figure 2.2). The hydrophobic tail (can be either straight or branched) of the surfactant molecule interacts more strongly with the oil molecules while the hydrophilic head has more affinity towards the water molecule (solvation). The solubility of the surfactant molecule depends on the hydrophilic to lipophilic ratio (HLB). This ratio characterizes the tendency of surfactant to solubilize in either oil or water and form water in oil or oil in water emulsions respectively. For instance, higher HLB results in the surfactant molecule being more soluble in oil system and forms water in oil emulsion (Paul Willhite. et al., 1998). Many such surfactant molecules combine together and form micelles. The oil molecules form the interior of the micelle while the exterior or the hydrophilic head of the micelle clings to the water molecules (Figure 2.3).

The hydrophilic head of the surfactant molecule is a characteristic parameter in defining the types of surfactant, classified as anionic, cationic, non-ionic and zwitterionic (Schramm. et. al., 2003).

Figure 2.2 Structure of a Surfactant molecule (Paul Willhite. et al. 1998)

Figure 2.2 above shows a surfactant molecule with its hydrophilic head and hydrophobic tail, while figure 2.3 below shows a micelle structure, once surfactant molecules unite. The micelles attribute toward forming micro-emulsions with low IFT values.

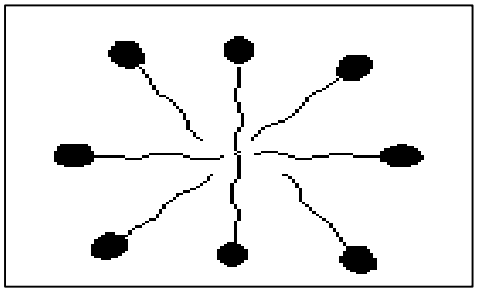

Figure 2.3 Structure of a surfactant micelle (Schramm. et al. 2003)

2.4.1. Types of Surfactants. Surfactants are classified on the basis of the ionic charge of the hydrophillic head of the surfactant as follows:

Anionic: As the name suggests anionic surfactants have a negative head group. These negatively charged surfactants help in lowering the IFT and can be manufactured economically. Their biggest advantage lies in their resistant nature to retention which can be attributed to the negative charge of the head group. As the head group is negatively charged, these surfactants repel against the negatively charged interstitial clay. Due to such advantageous properties, anionic surfactants are widely used in EOR techniques. Internal Olefin Sulfonate (IOS), an anionic surfactant, shows good tenacity against high temperature. Such surfactants can be used in reservoirs having high temperature since the stability of the surfactant will remain intact. A vast amount of research has been carried out on IOS surfactants as potential tools in surfactant flooding. Blending of various anionic surfactants to arrive at the best surfactant slug is an idea which has come forward in the 21st century. Levitt et al. studied a blend of IOS and propoxy sulfate and found promising laboratory results.

Non-ionic: These surfactants have a head group which has no ionic charge, hence the name non-ionic surfactants. These surfactants are generally used as co-surfactants, albeit after the chromatographic separation effects between the surfactants and the co-surfactants are studied. Common examples include alcohol, ester, ethers, etc.

Cationic: These are positively charged surfactants. These surfactants are occasionally used for EOR as they are adsorbed at the surface of interstitial clay due to the negative charge of the clay minerals and the positive charge of the

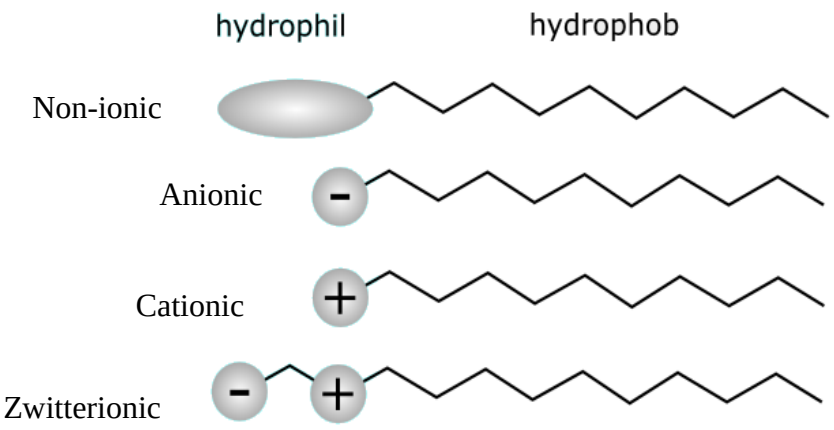

Figure 2.4 Types of Surfactants (Schramm et al. 2000)

surfactant molecule, this causes attraction between the two which results in loss of expensive surfactant from adsorption. The lower permeability reservoirs might add to their retention by phase trapping.

Table 2.2 Examples of different types of Surfactants (Schramm et al. 2003)

Class	Examples	Structures
Anionic		
	Na stearate	$CH_3(CH_2)_{16}COO^-Na^+$
	Na dodecyl sulfate	$CH_3(CH_2)_{11}SO_4^-Na^+$
	Na dodecyl benzene sulfonate	$CH_3(CH_2)_{11}C_6H_4SO_3^-Na^+$
Cationic		
	Laurylamine hydrochloride	$CH_3(CH_2)_{11}NH_3^+Cl^-$
	Trimethyl dodecylammonium chloride	$C_{12}H_{25}N^+(CH_3)_3Cl^-$
	Cetyl trimethylammonium bromide	$CH_3(CH_2)_{15}N^+(CH_3)_3Br^-$
Non-ionic		
	Polyoxyethylene alcohol	$C_nH_{2n+1}(OCH_2CH_2)_mOH$
	Alkylphenol ethoxylate	$C_9H_{19}–C_6H_4–(OCH_2CH_2)_nOH$
	Polysorbate 80 $w + x + y + z = 20$ $R = (C_{17}H_{33})COO$	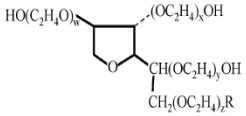
	Propylene oxide-modified polymethylsiloxane (EO = ethyleneoxy, PO = propyleneoxy)	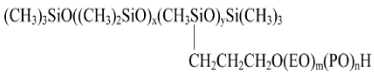
Zwitterionic	Dodecyl betaine	$C_{12}H_{25}N^+(CH_3)_2CH_2COO^-$
	Lauramidopropyl betaine	$C_{11}H_{23}CONH(CH_2)_3N^+(CH_3)_2CH_2COO^-$
	Cocoamido-2-hydroxypropyl sulfobetaine	$C_nH_{2n+1}CONH(CH_2)_3N^+(CH_3)_2CH_2CH(OH)CH_2SO_3^-$

Zwitterionic (Amphoteric): These surfactants have a negative as well as a positive group head as shown in figure 2.5. Zwitterionic surfactants are known for their robust structure, high tolerance to salinity and temperature (Alhasan Fuseni et al. 2013). Needless to say, these surfactants are used in harsh reservoirs and have immense potential for EOR in future. A healthy amount of research is already underway (Zhou Xianmin et al. 2012, Bataweel et al. 2012).

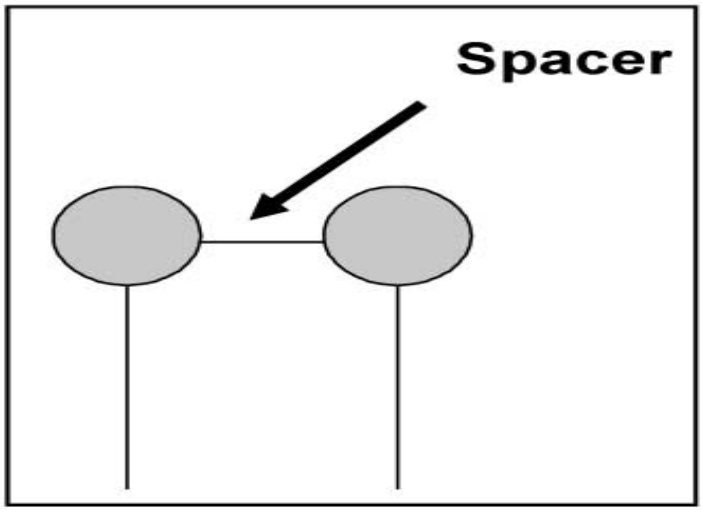

Figure 2.5 Diagram showing structure of Gemini surfactant molecule (Bo Gao et al.2013)

Besides these four general surfactant types, there also exist a few other less used surfactants like Viscoelastic surfactants (VES) and Gemini surfactants. Gemini surfactants are described as dimeric surfactants as the surfactant molecules have two head

groups and two tails per surfactant molecule, which are linked by spacer group (Shramm. et al. 2000). Developed in late 1980s and early 1990s, these surfactants can either be Cationic, Anionic, Non-ionic or Zwitterionic Gemini depending on the hydrophilic head of the surfactant molecule. The great advantage of Gemini surfactants over single-tail, single-head surfactants is that, they have low Critical Micelle Concentration (about an order of magnitude) (CMC) and can be used in low permeability reservoirs. They also exhibit high surface activity, better stability, low IFT at CMC and high hard-water tolerance. Figure 2.5 shows the basic structure of a Gemini surfactant molecule.

2.5 MICROEMULSION AND CMC

The term micro-emulsion was first used by Schluman et.al in 1977. These micro-emulsions form colloidal solution. The use of the word micro-emulsion was in debate after it was coined, Shinoda's and Kunieda's work stands a case in point. According to Healy and Reed, a micro-emulsion is defined as a stable, translucent micellar solution of oil, water that may contain electrolytes and one or more aphiphilic compounds (surfactant, alcohol) (Healy and Reed, 1974).

Micro-emulsions contain micelles that solubilize the immiscible phase with the solvent in the micro-emulsion solution. These micelles are called as swollen micelles. With the right amount of concentration of micro-emulsions, a significant amount of oil can be solubilized.

At low concentration of a surfactant in a solution, the surfactant molecules are dispersed randomly. These random surfactant molecules are called as monomers. However, as the concentration of the surfactant molecules increases, they start aggregating together to make the insoluble phase soluble. The coalesced surfactant

molecules form a sphere, like a droplet of a liquid substance, which are called as micelles. These micelles later form a micro-emulsion.

The micelles only start forming after a certain value of a surfactant concentration. This value is called the Critical Micelle Concentration of a given surfactant. Once, the concentration has reached CMC and micelles are formed, the surfactant monomers stop getting dispersed in the solution but start getting added into the micelles. This is an important phenomenon when surfactants are used in EOR techniques. This can be explained by stating that after reaching CMC the surfactant injection should be stopped as the added surfactant will only aggregate with micelles and not contribute to further IFT reduction. Adding more surfactant to the solution after achieving CMC will cause its wastage and increase the expenditure of the EOR project.

When a surfactant is added to the immiscible phases of water and oil, they form micelles which convert the immiscible phases into a single solution. The single solution formed can either be water in oil type or oil in water type. This helps in increasing the microscopic sweep efficiency. Microscopic sweep efficiency as the name suggests increases the mobility of the oil bank formed by the surfactant micelles on the scale of pore spaces. This simply means that the solution of water and oil moves with more ease in the pore spaces of the reservoir.

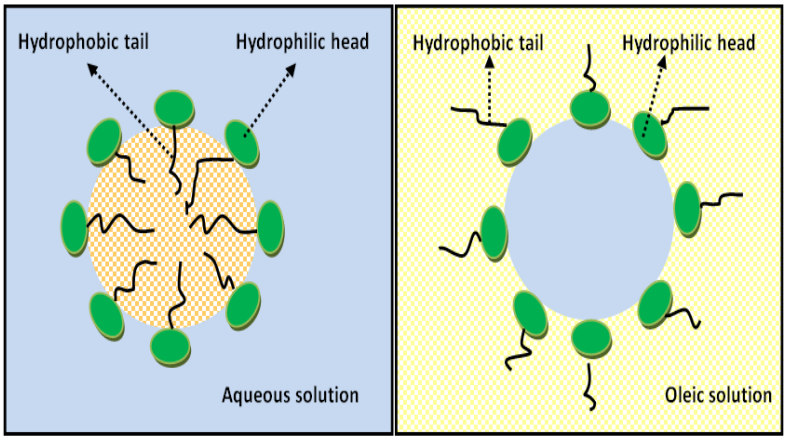

Figure 2.6 Micelles Left: oil-in water, Right: water-in oil (Paul & Willhite., 1998)

Figure 2.6 shows 2 different types of micro-emulsions a surfactant can form with the oil-water system, while figure 2.7 exhibits the formation of micelle at critical micelle concentration of surfactants.

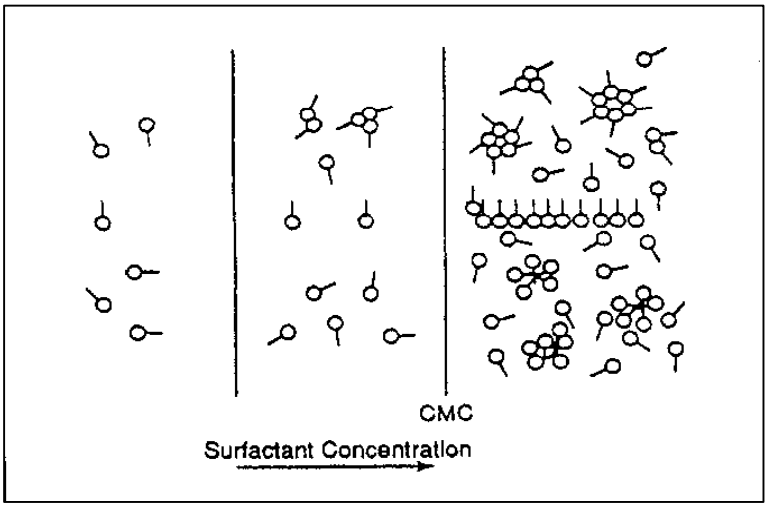

Figure 2.7 Formation of Micelles from monomers (Paul & Willhite., 1998)

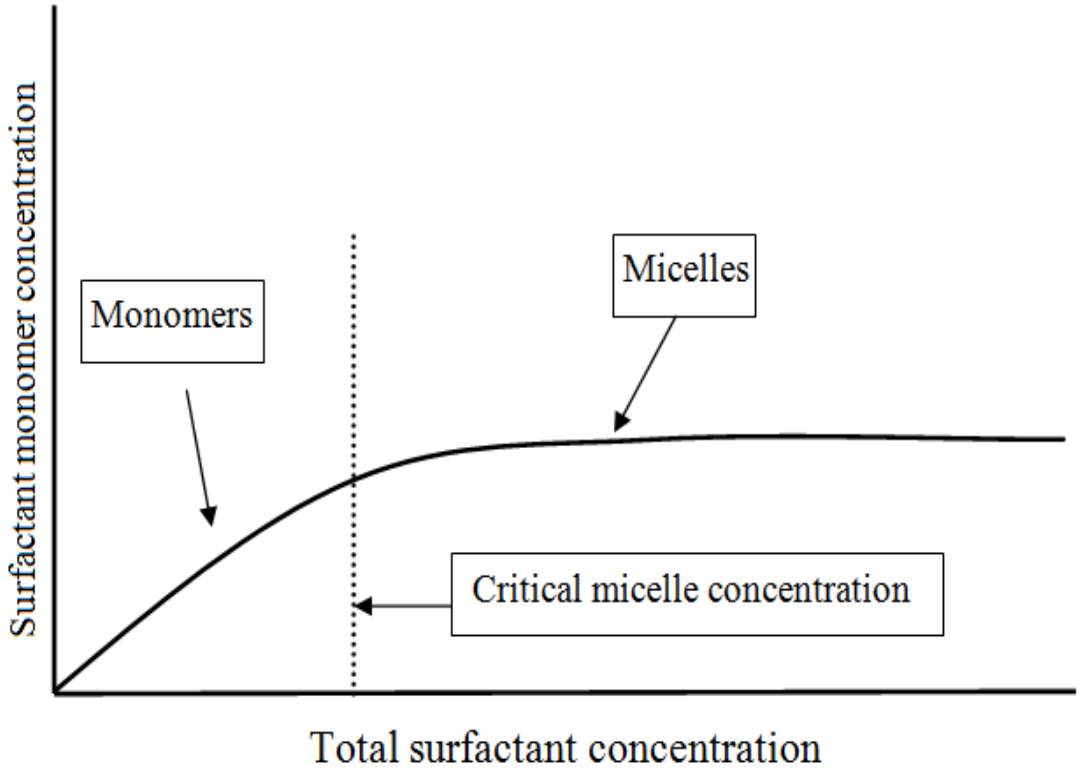

Figure 2.8 Graphical representation of relationship between CMC and Micelles

2.6 PHASE BEHAVIOR

Phase behavior studies of surfactants slugs to evaluate the robustness and IFT reduction capacity were carried out in the era of 1980s and 1990s (Puig J. E. et al. 1979, Hall A. C. 1980). Micro-emulsion systems between oil, water and surfactant can be designed which have ultralow IFT's (order of magnitude 10^{-3} dynes/cm). This is one of the mechanisms of surfactant flooding.

Phase behavior studies are tedious as the micro-emulsion systems are sensitive to the structure and concentration of surfactant slug (which includes surfactant, co-surfactant (usually an alcohol or another surfactant), oil and brine water), temperature and

pressure. Phase behavior studies evaluate regions where solubilization caused by micelles is maximum and the micro-emulsion is least affected by the above mentioned parameters. In literature, there are not any universally accepted mathematical equations which can be used to evaluate the phase behavior studies of surfactant. This results in laboratory evaluation of the micro-emulsions, where micro-emulsion structures are studied experimentally. The results obtained from the experiments are produced in the form of graphs which can be used in different computer softwares (for instance UTCHEM) to create mathematical model.

Healy and Reed in 1974 studied the phase behavior of surfactants with the help of ternary diagrams. The concept of ternary diagram was introduced on the basis of the principle that the micro-emulsion at least consist of three components namely, oil, water and surfactant. The most ideal system was considered to have these three phases after the equilibrium between the three components was achieved. The system with an ideal amount of all the three phases was a stabilized one. There exist three types of scenarios for a system. The type of system will depend on how the phase behavior changes take place while the three phases try to achieve equilibrium. These three types are Winsor type I, Winsor type II and Winsor type III. Winsor type I forms a lower phase equilibrium region, which means the lower phase micro-emulsion attains equilibrium with the oil above it. This type is also referred as Winsor type II-, where II means that two phases exist in the system. In this system the solubility of the surfactant is more towards the brine region (lower phase) as there is an electro-static force acting continuously between the surfactant ions and the uneven distribution of water dipole ($O^- H^{+)}$. The water dipole moment results in solubilization of surfactant in the brine region due to which IFT of the

system remains high. Only a small amount of oil is seen in the solubilized region. Winsor type II system exists when surfactants solubilize the upper phase region of the system with the lower excessive brine phase region. This type also has only two phases co-existing together. The lower region phase is purely aqueous with brine water and the upper solubilized phase with excessive oil. This type will not reduce the IFT adequately for the oil to be produced. Winsor type III shows a co-existence of water, oil and surfactant in the micro-emulsion. When the solution reaches type III state equilibrium is established between the three phases mentioned above and results in the formation of an oil bank in the middle region occupied by the micro-emulsion. Winsor type III is considered the most productive as it reduces the IFT to the least value when compared to the other 2 types. The varying salinity conditions from the optimal salinity requirement cause variations in the type III system.

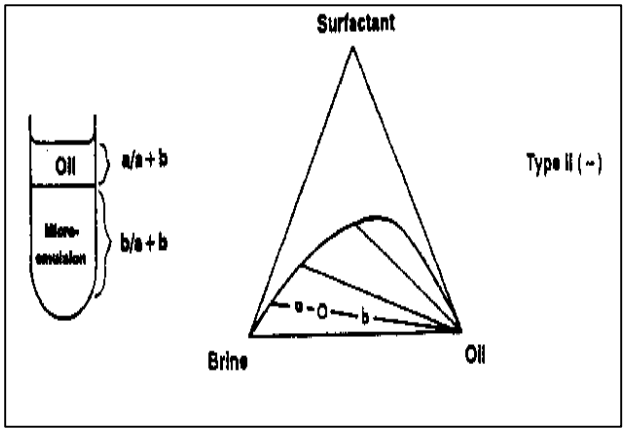

Figure 2.9 Winsor type I system (salager et al., 1979)

Figures 2.9, 2.10 and 2.11 show the winsor types behavior I, II and III respectively. Winsor type III behavior is considered the most ideal of the micro-emulsions a surfactant can form with an oil-water system.

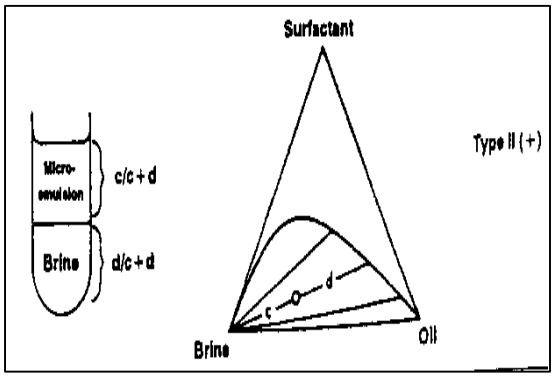

Figure 2.10 Winsor type II system (salager et al., 1979)

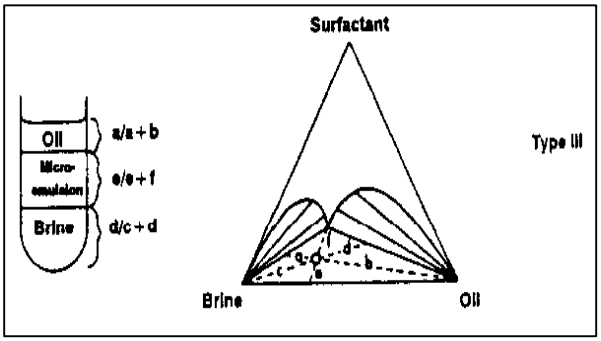

Figure 2.11 Winsor type III system (salager et al., 1979

Healy and Reed and Healy et.al. studied the effect of salinity on the phase behavior of a micro-emulsion. It was found that the stability of three phase micro-emulsion which has the lowest value of IFT exists only for a selected range of salinity and the mid-point of this range was the value called as optimum salinity value (S*). Optimum salinity gives the right amount of density to the micro-emulsion to solubilize required amount of water and oil in the middle region. However, if the salinity is more than the optimal salinity, the micro-emulsion region witnesses change from the required type III system and transform's into type I or type II with increase or decrease in salinity respectively (Figure 2.12)

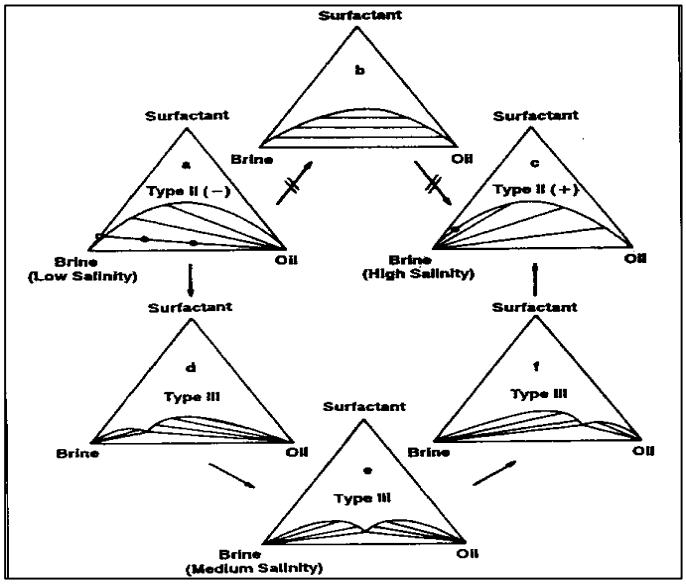

Figure 2.12 Effect of changing salinity on type III system (Paul & Willhite 1998)

Figure 2.12 as explained shows the effect of salinity on the Winsor type micro-emulsion formed by surfactants and figure 2.16 shows the actual test done to check the effect of salinity on the ability of surfactant to form micro-emulsions.

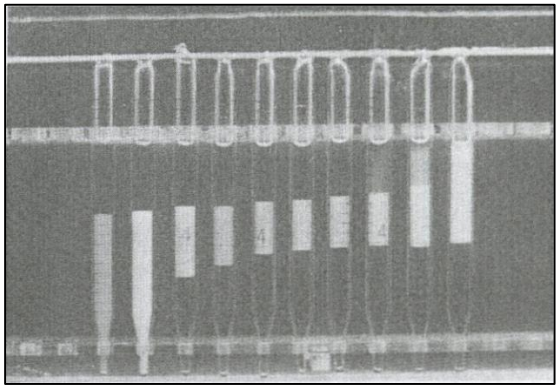

Figure 2.13 Micro-emulsion type changes with increasing salinity to the right (Ted Davis et al., 1980)

2.6.1. Phase Behavior Observation. Phase behavior testing is an important part of the screening process of surfactants. Phase behavior testing is carried out for a surfactant at a particular temperature, hydrocarbon and surfactant concentration.

Generally, a small quantity (usually 2ml) of sample of oil-water-surfactant mixture is pipetted into a long pipette (usually 5 ml) and then placed in an oven with a specific temperature set to match the reservoir temperature. After the temperature is reached the pipettes are inverted several times. The solutions in the pipettes are later studied to observe the phase behavior.

The solution is studied to observe the changes in the micro-emulsion region. It is also studied to observe the changes in Winsor types the micro-emulsion system goes through. The salinity is kept on increasing in small intervals to study the effect of salinity and parameters like Optimal salinity (S^*) and Solubilization ratio (σ^*) are measured through graphs. For a given system of oil-surfactant-water, solubilization ratio is the volume oil and water being solubilized by a unit amount of surfactant (Paul & Willhite 1998). Figure 2.14 from a DOE report of surfactant evaluation shows the graphical method of obtaining the value of S^* and σ^*.

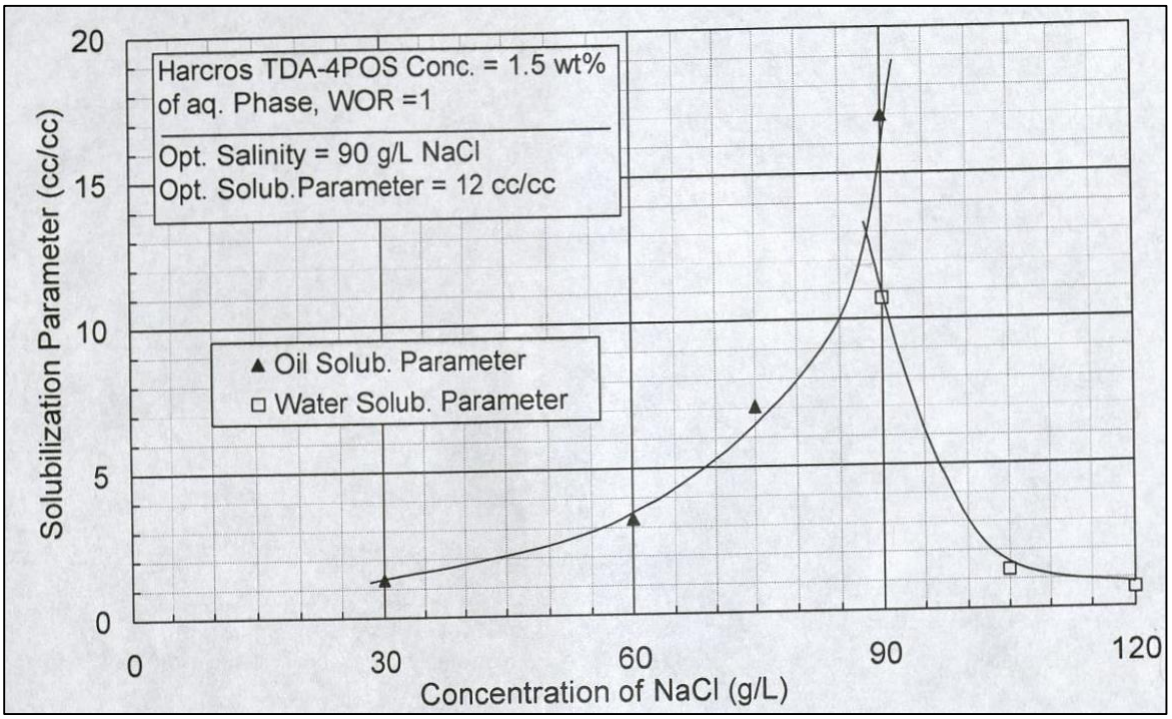

Figure 2.14 Solubilization and Optimal salinity graphs (Hirasaki et al., DOE report 2004)

2.7 SURFACTANT RETENTION

Surfactant retention occurs due to adsorption, phase trapping or precipitation. Adsorption of surfactants on the solid-substrate of the rock (especially in carbonate reservoirs) is one of the important factors in determining the success of a surfactant flooding process. A great amount of surfactant is lost due to adsorption which results in increasing the cost of the project and rendering the flooding impractical. In a typical project half or more of the total project expenditure is attributed to the surfactant cost (K. O. Meyers et al. 1981). Therefore, surfactant adsorption studies are imperative in a surfactant chemical EOR method project.

Surfactant retention by precipitation is generally caused by the temperature effects on the surfactants. Precipitation occurs due to the dissolution of surfactant elements into salts (Kleppe J and Skjeveland S.M 1992). Therefore it is essential to design a surfactant which is robust enough against dissolution in salt. Here, the pH of the surfactant plays a major impact on the resultant adsorption. Hardness which is generally considered as the concentration of divalent ions (Ca^{2+}, Mg^{2+}) also is an important parameter controlling the amount of surfactant adsorption. Diffusion of surfactants on pores of a rock (phase trapping) also causes surfactant retention (Cuong T. Q Dang et al., 2011).

Adsorption mainly occurs due to the charged head groups of solid surface and the charged hydrophilic head of the surfactant (Figure 2.15). Generally, a single monomer of surfactant is adsorbed on the rock surface rather than micelles being adsorbed as a whole. (Somasundaram et al., 2000). Adsorption of surfactants depends on the surfactant type, concentration, molecular weight, pH, salinity and importantly on reservoir heterogeneity.

Langmuir adsorption isotherms (or simply adsorption isotherms) are used right from 1980's (EOR boom period) till today (J. F. Scamehorn et al., 1980, Cuong T. Q

Dang et al., 2011). The isotherm curve is a plot of Surfactant adsorption Vs Surfactant concentration.

These curves generally show a steep rise in the surfactant adsorption, occurring when the surfactant is in the Winsor type I and type II region. Once, the surfactant concentration hits the CMC value, the adsorption remains fairly constant as shown by most of the curves. This region is called a plateau and is of considerable importance. The CMC value is usually 100 times more than the surfactant concentration at the start of injection and the aim of adsorption isotherms is to note the adsorption value at the CMC since this is the highest adsorption value the surfactant slug attains. Hence, these factors suggest that the shape of the curve below CMC value has little impact on the total surfactant adsorption (Cuong T. Q Dang et al., 2011).

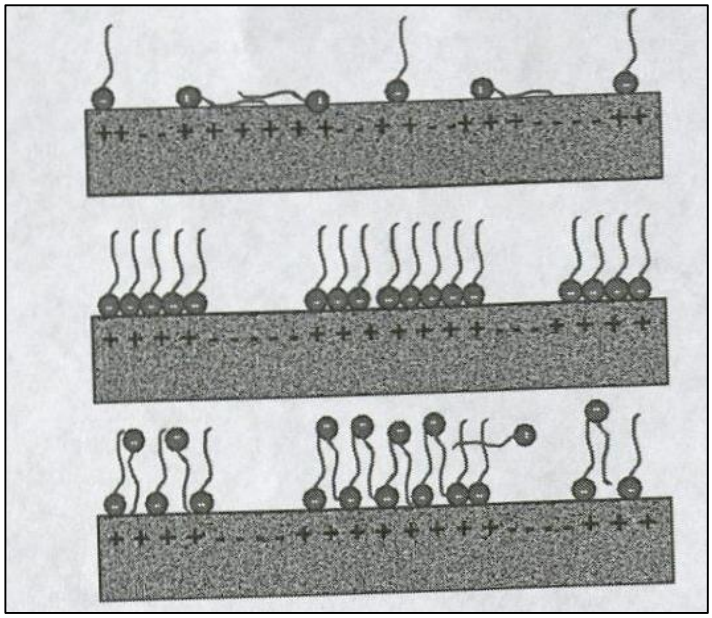

Figure 2.15 Surface adsorption on the rock surface (Cuong T. Q Dang et al., 2011)

The aforementioned adsorption curve is derived from the experiments carried out in the laboratories, where a surfactant under test is exposed to the reservoir rock (either crushed or in the form of a core). Static adsorption method comprises of crushed rock pieces being placed in a small tubes along with surfactants. The temperature is varied to notice its role in surfactant adsorption. The liquid/solid system is then well mixed by centrifugation and random hand agitation.

Dynamic adsorption method consists of rock cores being flooded with surfactant slug to study the adsorption. The surfactant concentration is gradually increased until CMC is reached and the curve shows a remarkable plateau.

2.8 SURFACTANT MECHANISMS

Surfactants reduce the IFT between oil and water by emulsifying them. It also results in wettability changes from oil wet to water wet used in surfactant imbibition EOR in fractured carbonate reservoirs. Reduction in IFT results in an enhanced microscopic displacement efficiency. To have a desired volumetric sweep efficiency (mobility control), polymers are added after injecting surfactants. This method is called as Surfactant/Polymer EOR.

2.8.1. Interfacial Tension. Interfacial tension or IFT is the contractile tendency at the liquid-liquid interface (for instance oil/water) when the two immisicible liquids are in contact. It is the force per unit length which is required against the contractile forces to create more surface area (Paul & Willhite, 1998). In reservoir rocks the oil and brine IFT is between 20-30 dynes/cm as shown in figure 2.16. Due to such high IFT the residual oil saturation and remaining oil saturation of the reservoir is higher. Surface active agents like surfactants can be used to reduce the IFT by creating more surface area at the

junction of the two liquids. This will increase the microscopic displacement efficiency of the reservoir and reduce the residual oil saturation.

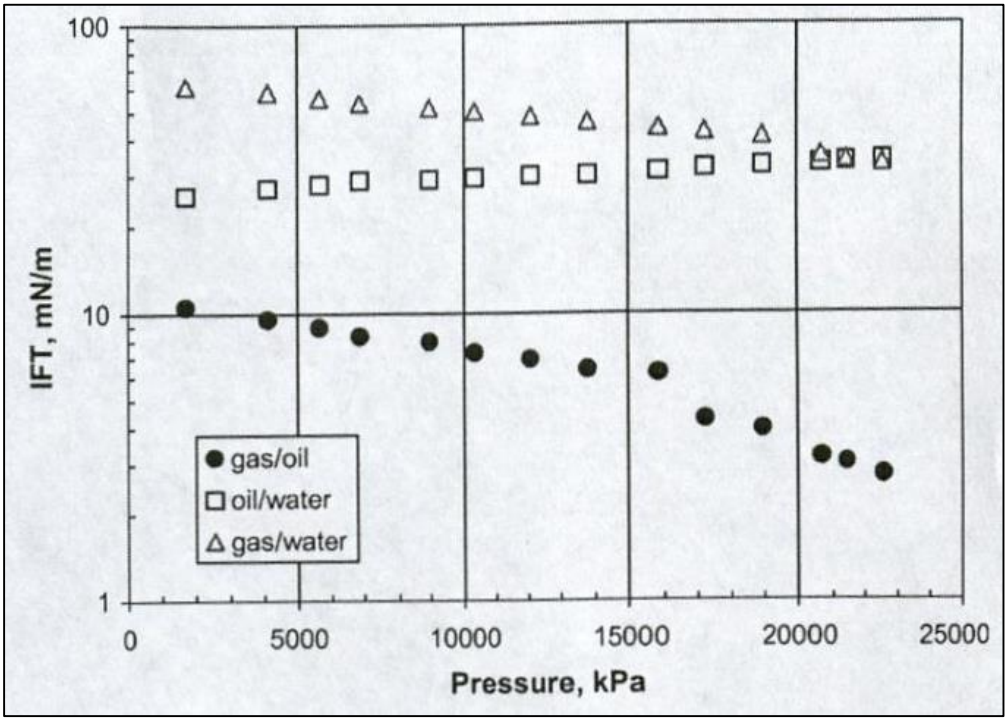

Figure 2.16 IFT between Oil, gas and brine phases (Yildiray Cinar et al., 2005)

Capillary number is the ratio of viscous forces over capillary forces (Saffman and Taylor 1958). In literature, there are many other definitions of capillary number. Mathematically it is denoted by N_c.

$$N_c = v\mu/\sigma$$

Where:

N_c is capillary number

V is the effective velocity

μ is the viscosity of the displacing fluid

σ is the IFT between oil and water

CDC is an ideal method to co-relate residual oil saturation to the physical properties (like capillary forces, IFT) on a microscopic sclae (pore scale) (Bashiri A. et al., 2011). Taber in 1979 showed that, the inversely proportion relationship between capillary number and IFT can be used as a method to decrease the residual oil saturation. CDC which show that when capillary number is increased the residual oil saturation decreases. He also suggested that the capillary number of the reservoir system after waterflooding is somwhere close to 10^{-7}. The low value of capillary number after waterflooding can be increases if surfactants are used in the water system (LTWF) which will reduce the IFT of the system and in turn increase the capillary number. CDC are plots of ROS Vs N_c as shown in the figure 2.17.

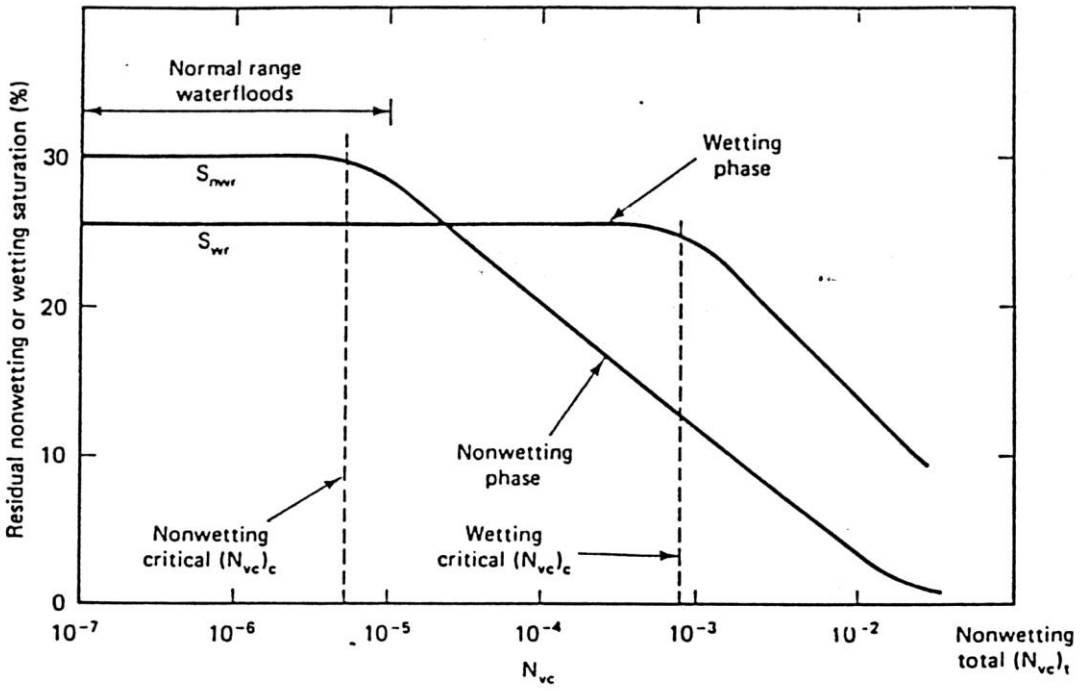

Figure 2.17 Capillary Desaturation Curve (CDC) (Lake, 1989)

The viscous forces, directly proportional to the capillary number depend on the permeability of the reservoir, the applied pressure drop and the viscosity of the displacing fluids while the capillary forces depend on the IFT of oil and water, wettability conditions and pores geometry (M. Delshad et al., 1986). The aforementioned parameters on which the viscous and capillary forces depend suggest that increasing the viscous forces to increase the capillary number is not feasible (for instance, there is always a danger of damaging or fracturing the formation if the viscosity of the displacing fluid is more than the fracture pressure of the formation. IFT is measured with the help of spinning drop tensiometer (V.J. Kremesec et al., 1988).

2.9 SURFACTANT FLOODING AND TYPES

Surfactant flooding Surfactant flooding is broadly classified into two namely, Micellar-polymer (Surfactant polymer flooding) and Alkaline-Surfactant-Polymer flooding (ASP) (Paul & Willhite, 1998). Any deviation from the aforementioned methods is subtle, for instance, surfactants can be added to water while waterflooding to decrease the capillary forces between the injected water and oil resulting in better recovery efficiency. This method is called as low tension water-flooding (Gogarty W.B., 1978). Second subtle change from the main method is by adding foam instead of polymer for mobility control purposes.

Despite of few subtleties, the above mentioned two methods remain the imperative methods which have been piloted and also implied on a large scale in a few reservoirs. These surfactant flooding methods and their application is described extensively in the following sections.

2.9.1. Micellar/ Polymer Flooding. A micellar/polymer flooding operation employs a micellar solution consisting of oil, water, surfactant and small amounts of other chemicals like, co-surfactants (alcohol, other surfactants) polymer. These chemicals together make the micellar/ polymer flooding slug. This method is also called as Micro emulsion flooding and Surfactant-polymer flooding (Sara T. et al., 1992).

A Micro-emulsion of oil/surfactant/water exists in the form of drops of the size of microns. Hence, this method improves the microscopic efficiency of the reservoir. Micellar/polymer method was first used and patented for Marathon oil co. by Gogarty and Tosch known as Maraflood. The injection profile of the method consists of injecting a pre-flush (to achieve the desired salinity environment), followed by micellar slug

(surfactant, co-surfactant, electrolyte), which is followed by polymer solution along with drive water. Figure 2.18 below shows the injection profile of the flooding method.

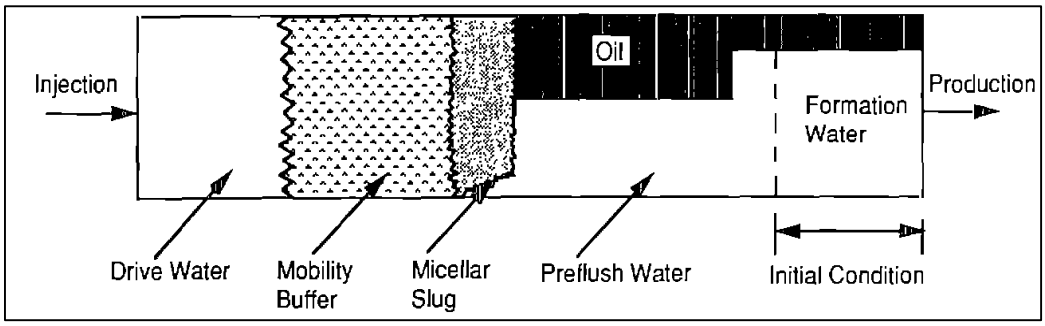

Figure 2.18 Micellar/ Polymer flooding injection profile (Sara T. et al., 1992)

The method establishes low IFT between oil and water and forms an oil bank which is eventually produced.

2.9.2. Alkaline Surfactant Polymer (ASP) Flooding. Alkaline surfactant flooding method comprises of injecting alkaline (NA_2CO_3, KOH) followed by surfactant and polymer. The main objectives of the method are to reduce the loss of surfactants by retention, changing the wettability and reducing the IFT of the fluids. Alkaline chemicals reduce the surfactant retention, increase the pH value and also react with the acidic content of hydrocarbons (Naphthenic acids) to generate more surfactants in the reservoir. The intensity with which the alkaline substance reacts with the acids depends on the acid number of the hydrocarbons. The Polymer noticeably is used to improve the mobility

conditions. They provide the necessary volumetric efficiency to the system. Extensive research is been carried out in ASP methods at the turn of 21st century. Field applications are noticeable in the USA and on a large scale in China.

$$HA + OH^- \rightarrow A^- + H_2O$$

Where, A- is the soap component formed

HA- Naphthenic acid component

2.10 SURFACTANT EVALUATION

Screening criteria of any EOR method is considered as the first step towards evaluating a successful EOR project. Virtually since three decades, EOR techniques have been evaluated as new technologies emerge in the EOR industry. Due to this emergence in technology it is critical to always keep the screening criteria updated. Screening criteria is extremely important as the first step to any EOR evaluation as a massive amount of money is invested to apply an EOR method. Hence, to avoid the risk of a failure every EOR method is carefully evaluated for a particular set of oil and reservoir properties (Hite 2004). The objective of a screening criteria operation is to impeccably estimate a specific range on reservoir and oil properties in which various EOR methods are applicable (Paul & Willhite, 1998).

Surfactant evaluation is carried out to test the efficacy of a single surfactant or a mixture of various surfactants. Surfactant structure, concentration and suitable values of oil properties like oil viscosity, brine salinity, reservoir temperature, formation mineralogy are various parameters for which the surfactant is evaluated (Hirasaki et al.,

2004). The surfactant type is hampered and limited by the reservoir temperature and salinity (Paul and Willhite, 1998).

According to Hirasaki et al., surfactant evaluation must take into account the chemical/physical conditions in reservoirs, economic factors, commercial availability of surfactants and type of surfactant method applied. It is important to evaluate the surfactant to check its interaction with the type of reservoir rock. For instance, the physical properties of the sandstone rock vary when compared with carbonate rocks. Hence, different surfactant methods are evaluated for these rocks. Sandstone rocks are generally not fractured while carbonate reservoirs mostly have a fracture network. Surfactant imbibition method is evaluated for carbonate rocks. It is also important to know the aqueous phase chemistry of the reservoir and its interaction with surfactant. In order to study the aforementioned relationship, surfactants are characterized by the optimal salinity (S*) (at which the surfactant are the most stable) for different hydrocarbon specimen. Solubilization parameter estimates the level of IFT reached at the optimal conditions. In surfactant evaluation, surfactants are monitored for formation of viscous gel or liquid crystals which change the micro-emulsion composition and hamper favorable IFT values and eventually the recovery factor.

Over the past 20 years, many researchers have developed and published technical screening criteria for different EOR techniques. Table 2.3 shows the screening criteria for surfactant flooding published by different researchers. The EOR screening studies presented by Brasher and Kuuskraa (1978) had a dataset of 200 EOR pilot projects in the USA. They analyzed the data from both a technical and an economic perspective. Carcoana (1982) presented screening criteria for some EOR techniques; these criteria

were based on the pivotal knowledge of reservoir properties and the results obtained from commercial applications of EOR techniques in Romanian oil fields. Taber (1983, 1997) proposed screening criteria based on field data and oil recovery mechanisms for commonly applied EOR techniques. This study considered the 1996 Worldwide EOR Survey to summarize the criteria. Taber's criteria that are relevant surfactant flooding include that the maximum oil viscosity should be less than 35 cP, and reservoir permeability should be greater than 10 md. He presented these screening criteria both graphically and in tables. Goodlett et al. (1986) presented screening criteria based on a summary of previously published screening criteria for chemical, gas injection, thermal, and microbial EOR techniques. Al Bahar et al. (2004) illustrated criteria for each EOR technique based on the literature and his own experience. He utilized software to evaluate the suitability of these criteria for EOR processes at 81 reservoirs in Kuwait. In addition, a novel improved hydrocarbon recovery (IHR) screening methodology has been developed to identify the appropriate process for any number of reservoirs. (Table 2.3 & Table 2.4 show only the criteria for Surfactant-Polymer flooding). Subsequently, a range for field and laboratory data was established considering the reservoir and fluid parameters. The work also included salinity and hardness parameters for which are imperative for chemical flooding. Also, the laboratory dataset included parameters such as IFT, surfactant adsorption and surfactant concentration which are important in defining the success of surfactant-polymer flooding.

Table 2.3 Screening guide for surfactant-polymer flooding

Author	Published year	Oil Gravity, °API	Oil Viscosity, cP	Oil Saturatioin Start, %	Permeability, md
Brashear	1978	>25	<20	25	>20
Carcoana	1982	>25	<30	30	>35
Peter H.	1984		<30		>40
Goodlett	1986	>25	<30	30	>40
Taber	1997	>20	<35	>35	>40
Al-Bahar	2004				>50
Aldasani & Bai	2010	22-39	3-15.6	43.5-53	50-60

Table 2.4 Screening guide for surfactant-polymer flooding

Author	Porosity, %	Temperature, °F	Depth, ft	Salinity, ppm	Hardness, ppm
Brashear	>20	<200		<50,000	<1000
Carcoana	>20	<180	<7000		
Peter H.		<200		<100,000	
Goodlett	>20	<200	<9000	<140,000	
Taber		<200			
Al-Bahar		<158		<50,000	<1000
Aldasani & Bai	16-16.8	122-155	625-5300		

3. RESULTS AND DISCUSSIONS

A dataset consisting of Surfactant-Polymer field projects (Micellar-Polymer, Micro-emulsion projects) from worldwide EOR survey biennially published in the Oil & Gas Journal was established. The authenticity of the data collected from the Oil & Gas Journal was verified from SPE publications on the respective projects. Eventually, the dataset acquired consisted of 42 field projects. Additionally, the study comprised of dataset from laboratory work carried out in surfactant-polymer flooding. The laboratory dataset consisted of 200 experiments which were acquired from SPE literature (onepetro) dedicated toward these experiments. The following work explains the data analysis and range established from the acquired field and laboratory dataset.

3.1 FIELD PROJECTS

3.1.1. Data Cleaning. The quality of data collected plays a major role in establishing a genuine screening criteria result for any EOR process. The collected data might contain problems that can affect the quality of dataset, in particular, duplicate projects, missing data, inconsistent data and special cases.

The problem of duplicate and inconsistent information in the dataset was solved by referring to the SPE work published on the field projects. All the published work referred therefore, provided an authentic dataset of field projects free from inconsistent and duplicate information. The special cases were however, analyzed by studying the relationship between box-plots and cross-plots for the different parameters.

Finally, the distribution of Surfactant-Polymer flooding projects applied in different countries is shown in figure 3.1. It can be conferred from the figure that approximately 79% of the field projects were applied in USA.

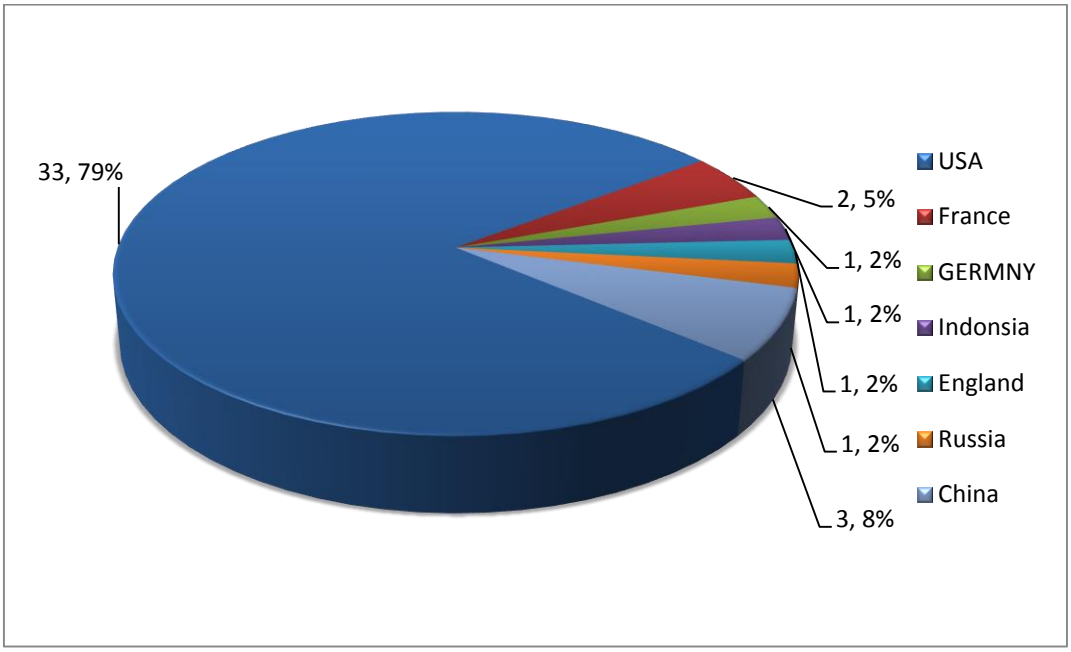

Figure 3.1 World surfactant-polymer flooding projects (From Oil & Gas Journal EOR surveys)

The remaining 9 field projects were applied in Germany, France, Indonesia, England, Russia and China with 3 field projects in China, 2 in France, while the remaining countries conducted 1 field project each.

3.1.2. Missing Data. Some fields in the dataset were missing one or more pieces of information. The missing data included °API gravity, Oil Saturation (start and end), salinity and hardness. Table 3.1 shows details of the missing information which were ignored in the analysis.

Table 3.1 shows the aforementioned parameters which were missing in the field projects in the dataset. It provides with the percentage value of each missing parameters along with the number of available and unavailable data for the same parameters. Brine hardness had the most amount of missing data with the percentage of 69.00%.

Table 3.1 Data unavailable for each parameter in the dataset

Parameter	Data available	Data unavailable	Data missing Percentage
Oil gravity (°API)	39	3	07.00%
Brine Salinity	23	19	45.00%
Brine Hardness	13	29	69.00%
Oil Saturation (Start)	36	6	14.00%
Oil Saturation (End)	18	24	57.00%
Depth	41	1	2%
Oil gravity (°API)	39	3	7.00%
Porosity (%)	41	1	2

3.1.3. Data Problem Detection. The dataset was analyzed for special cases and a few inconsistent data. To interpret these problems, basic diagrams viz. box plots and cross plots were used.

Box-Plot: In descriptive statistics box-plot is a quick and efficient way to analyze the data. It helps in visually summarizing the data and spot the special cases. The special cases for a given parameter are the values which lie segregated from the majority of the data-points. The box-plot also gives the range of the values which fall between the minimum and maximum limit. It is divided into 5 parts. The characteristic features of a box-plot can be explained as follows.

1. The lowest value (minimum)
2. The highest value (maximum)
3. The mean value (Average data value)
4. The first quartile (25^{th} percentile)
5. The second quartile (50^{th} percentile)
6. The third quartile (75^{th} percentile)

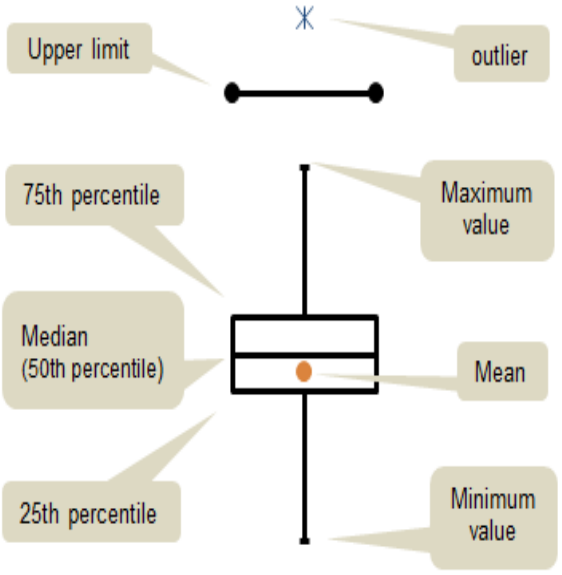

Figure 3.2 Schematic of a box-plot

Figure 3.2 is a depiction of a box-plot with its characteristic features. The figure explains the concept of special cases, which are values larger and smaller than the upper and the lower limit of the data respectively. The upper limit of the data is calculated as 1.5 the interquartile range plus the 75^{th} quartile, while the lower limit as 1.5 times the interquartile range minus the 25^{th} quartile. The interquartile range is the difference between the 75^{th} quartile and the 25^{th} quartile. The mean is the dot at the center of the plot.

Cross-Plot: A Cross-plot is an X-Y plot which is used to interpret a relationship between two different parameters. It is a plot with scattered points which follow a specific trend. Hence, a trend-line is achieved which shows the trend of the scattered data of the two parameters. A cross-plot combines well with the box-plots of the two

parameters and helps in better understanding of the data-points which lie separated from the majority of the points.

Figure 3.3 shows a cross-plot of temperature vs. depth to the left and temperature box-plot to the right. Generally, the temperature of a formation depends on the depth with temperature increasing with depth as the geo-thermal gradient increases with depth.

It can be inferred from the box-plot of temperature (figure 3.3, right) that all the temperature values of the fields lie below the upper limit of 214.75 which is denoted by the solid black line. These values did not show inconsistency with depth as shown in the cross-plot of temperature vs. depth. The upper limit in the temperature box-plot exceeded

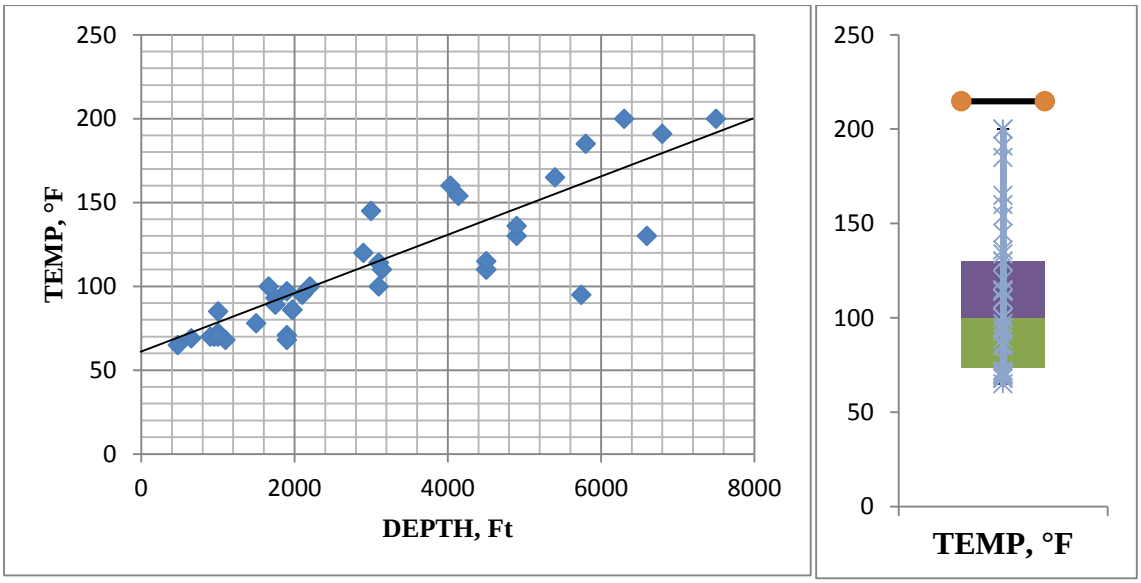

Figure 3.3 Cross-plot of reservoir temperature vs. depth (left) and temperature box-plot (right)

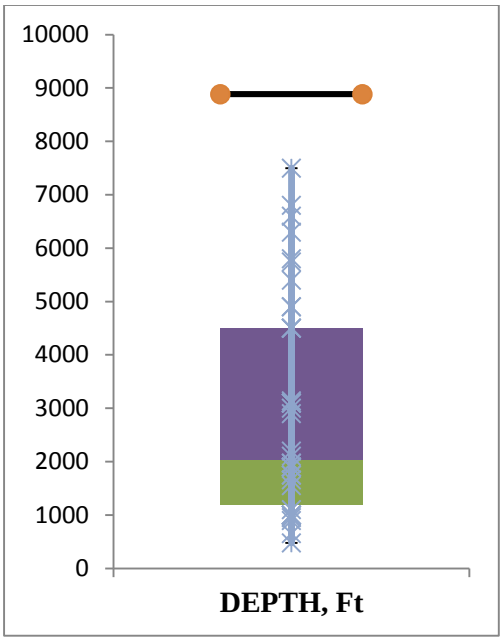

Figure 3.4 Box-plot of Depth

the maximum value of the temperature due to the mathematical formula of [Q_3+1.5*(interquartile)] by which it is calculated. The field project applied in Sloss area of Nebraska was considered as a unique project for its high temperature value. The other 2 temperature values of 191°F and 185°F close to the maximum value were recorded for the reservoirs in Arkansas. The field names were Wesgum and Lewisville respectively. Figure 3.4 depicts the box-plot of the reservoir depths for 40 field projects with the maximum value of 7500 feet and a minimum value of 475 feet. The maximum value was recorded for the field of East Coalinga Extension in California, USA while the minimum value was for St. Johnson field of Illinois, USA.

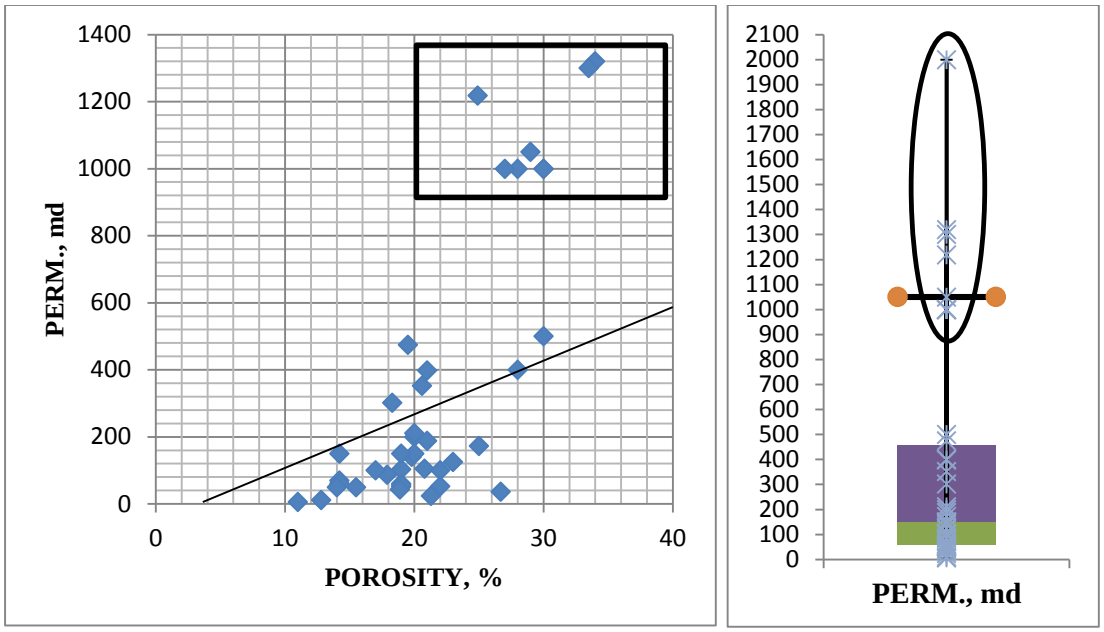

Figure 3.5 Cross-plot of porosity vs. permeability (left) and permeability box-plot (right)

Figure 3.5 above shows a cross-plot relationship of porosity vs. permeability to the left and the permeability box-plot for permeability values in the dataset. Values of 5 field projects exceeded the upper limit value of 1050.3md. These field projects were applied in Bell Creek, USA (2 field projects) and three field projects in China (2 in Shengli and 1 in Bohai Bay) with permeability values of 1050, 1218 for Bell Creek field and 1320, 2000 and 1300 md for oil fields in China respectively. Three field projects of viz. Chateaurenard, (France), Westblock 4 in Germany and Handil oilfield in Indonesia had reservoir permeability values of 1000md, approximately 50md less than the upper limit. However, these values were still higher than the permeability values for the majority of field projects. All these projects were conducted in unconsolidated sand formations which are highly permeable. These were the special cases which were not

included in defining the final range of permeability for SP flooding as all the other projects were carried out in sandstone reservoirs. Figure 3.6 shows a porosity box-plot for forty one porosity values. The upper limit and the lower limit of the plot are depicted, with the upper limit above the maximum value whisker and lower limit below the minimum value whisker.

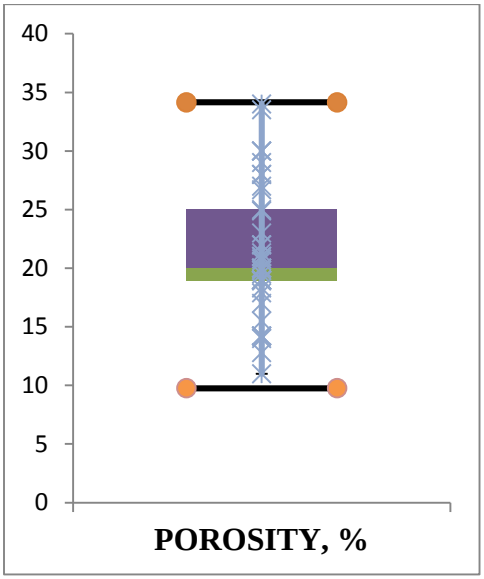

Figure 3.6 Reservoir porosity box-plot.

The porosity box-plot showed a wide spread between 11 and 34%. The upper and lower limit of the plot was higher than the maximum and lower than the minimum values respectively. This was attributed to the formula with the help of which these values are calculated.

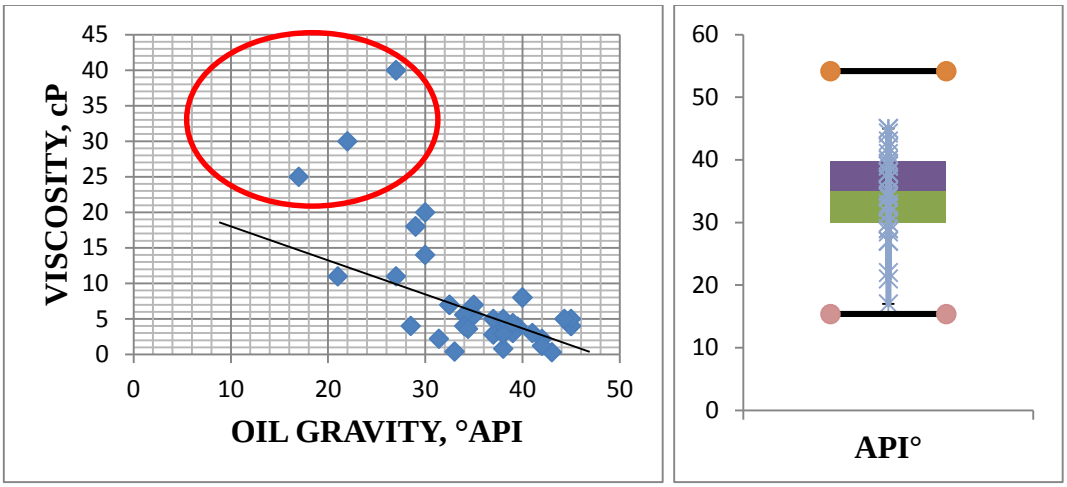

Figure 3.7 Cross-plot of oil viscosity vs. oil gravity (left) and oil gravity box-plot (right)

Figure 3.7 shows a cross-plot between oil viscosity and oil gravity and oil gravity box-plot to the right. Three oil viscosity values lie away from the trend shown by the majority of the values. These values of 40 cP, 25 cP and 30 cP were of the field projects applied in Chateaurenard, France and Willmington, USA. Bohai Bay off-shore project was conducted for oil viscosity of 30 cP. Chateaurenard reservoir had a high viscosity oil as the oil had no dissolved solution gas which made the oil thick. The oil also contained a large amount of paraffinic content. Similarly, the oil in Willmington reservoir was stripped of solution gas. The waterflooding history of the reservoir also attributed to the increase in viscosity of the oil. Since, low temperature water was injected in the reservoir during waterflooding, the temperature of the reservoir dropped considerably thereby, increasing the viscosity of the oil.

Similarly, it can also be inferred from figure 3.8, which is box-plot of oil viscosity, that two field projects with reservoir oil viscosity of 25, 30, 40, 45 and 50 cP.

These values were higher than the upper limit of 24.0785 cP with a maximum value of 50 cP observed in the Shengli oilfield (Northwest block) in China.

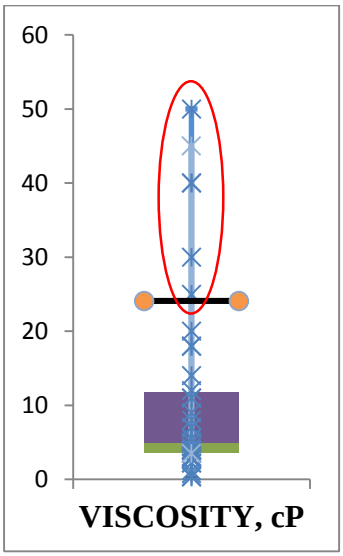

Figure 3.8 Oil Viscosity box-plot

Figure 3.9 and figure 3.10 show box-plots for Brine salinity and brine hardness respectively. Brine Salinity values showed a wide range from 400ppm to a maximum of 160,000ppm. Field projects in Loudon, Wichita and Manvel reservoir of USA had high salinity values than the majority of the values in the dataset. A minimum value of 400ppm was of the reservoir brine of Chateaurenard, France oilfield. The upper limit was calculated to be 175,350ppm which was

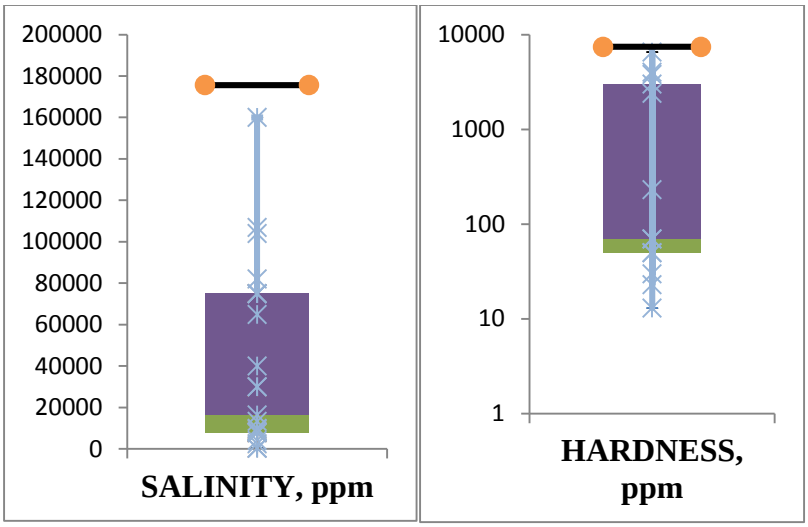

Figure 3.9 and 3.10 Box-plot of brine salinity (left) and brine hardness box-plot (right)

Figure 3.10 is a box-plot of brine hardness vs. brine salinity and a box-plot of brine hardness to the right. As seen from the box-plot 8 values from the 13 brine hardness values lie in the range of 13-231 ppm. Five hardness values were observed to be above 1000ppm. Three of these values are of the field projects applied at Salem, North-Burbank and Manvel all in the USA, with the brine hardness values of 3800, 6530 and 2400 ppm respectively. Brine hardness value of 3000ppm and 4000ppm were observed in the fields of Eldorado and Loudon located in Kansas and Illinois states of the United States. Brine hardness is the concentration of divalent ions (Ca^{2+} and Mg^{2+} in the brine). Brine hardness is an important parameter and has to be studied as high concentration of divalent ions in the brine results in the precipitation of the surfactant slug and affects its stability. This eventually, increases the cost of the entire Surfactant-Polymer flooding project.

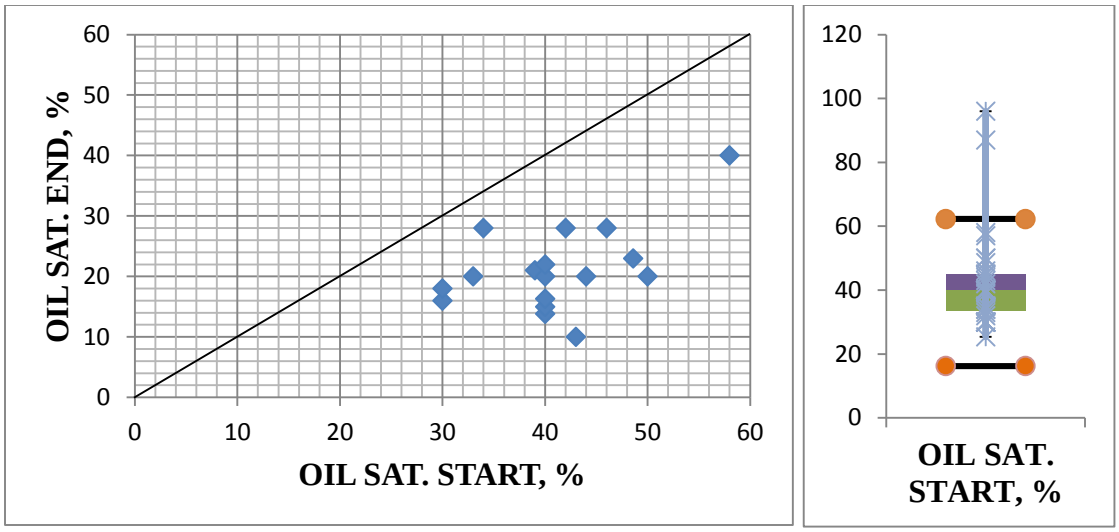

Figure 3.11 Cross-plot of oil saturation (start) vs. oil saturation (end) (left) and Oil saturation (start) box-plot (right)

Figure 3.11 shows a cross-plot of oil saturation (start) vs oil saturation (end) and a box-plot of oil saturation start values in the dataset. Also, figure 3.12 shows a box-plot of oil saturation end values. On the X-axis we have the oil saturation start value and on the Y-axis, oil saturation end values were plotted. The cross-plot has a line which passes from the minimum value of 0 to the maximum value of 60. Any point over this line would mean that the oil saturation end value is more than the oil saturation value at the start of Surfactant-polymer project, which cannot be possible. It can be inferred from the cross-plot that no project showed such inconsistency. However, the Surfactant-polymer project applied at the Botthamsall field in the United Kingdom shows a high final oil saturation value of 50% (also seen in the box-plot- Figure 3.12). This was attributed to the low permeability of the reservoir (6md) which caused high retention of the chemical slug. The box-plot of Oil saturation start shows 2 field projects in Arkansas- USA with

values of 87% and 96%. These high values suggest that the water-flooding recovery from these reservoirs was low.

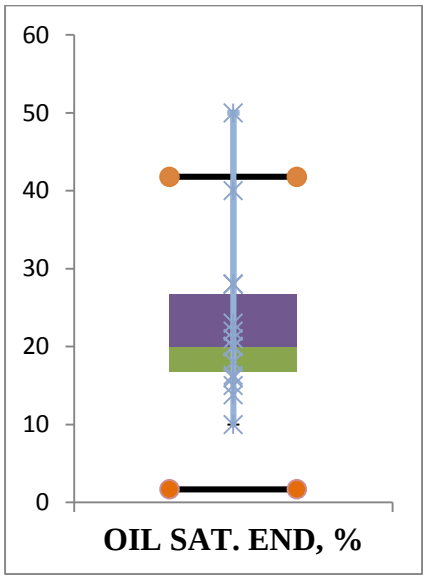

Figure 3.12 Box-plot of Oil saturation (End)

3.1.4 Methods to Display Data. After analyzing the data for special cases and consistency for different parameters, the dataset values were displayed with the help of histograms and box-plots.

Histograms: Histograms are used to display dataset values graphically and show data points in specified ranges. They also show the frequency of the data on the Y-axis and the parameters being measured on the X-axis.

Figure 3.13 shows a histogram of reservoir temperature of the dataset. It shows that the Surfactant-polymer chemical flooding is implemented in different ranges of reservoir temperature from 65-200°F. It also shows that the minimum value of reservoir temperature at which surfactant-polymer flooding method was implemented at 65°F, while highest was at 200°F. The highest peak was observed between 65-80°F. Approximately, 71% of the temperature values lied between 70-120°F.

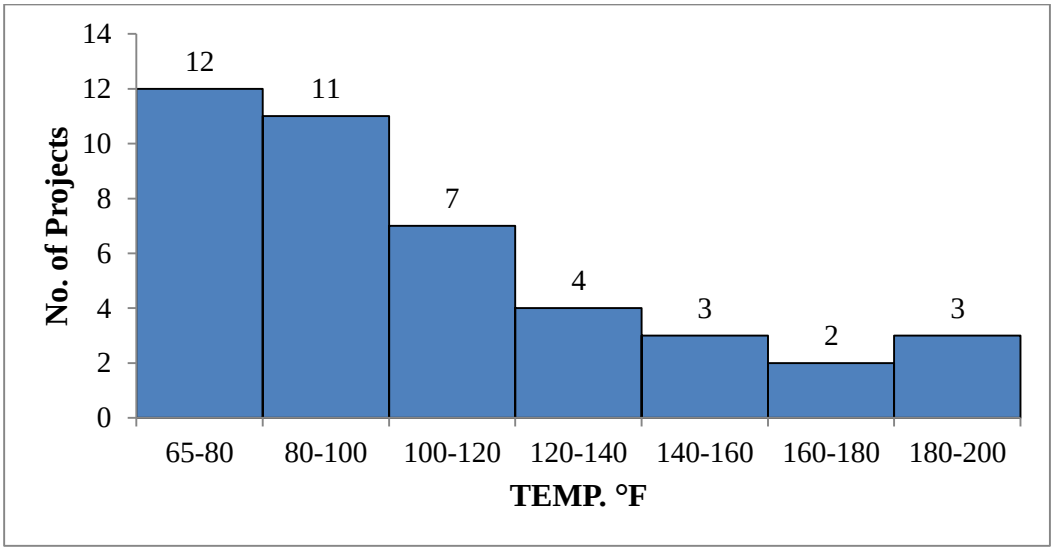

Figure 3.13 Reservoir temperature range of the dataset

Figure 3.14 below shows a histogram of reservoir depth for 41 surfactant-polymer chemical flooding projects. The figure shows that the peak for reservoir depth is between 1000-2000 feet. The majority of the values fall between the reservoir's depths of 500-

2000 ft, with more than 50% of the values falling in this range. Only 1 project lies between the highest value range of 7000 and 7500 ft.

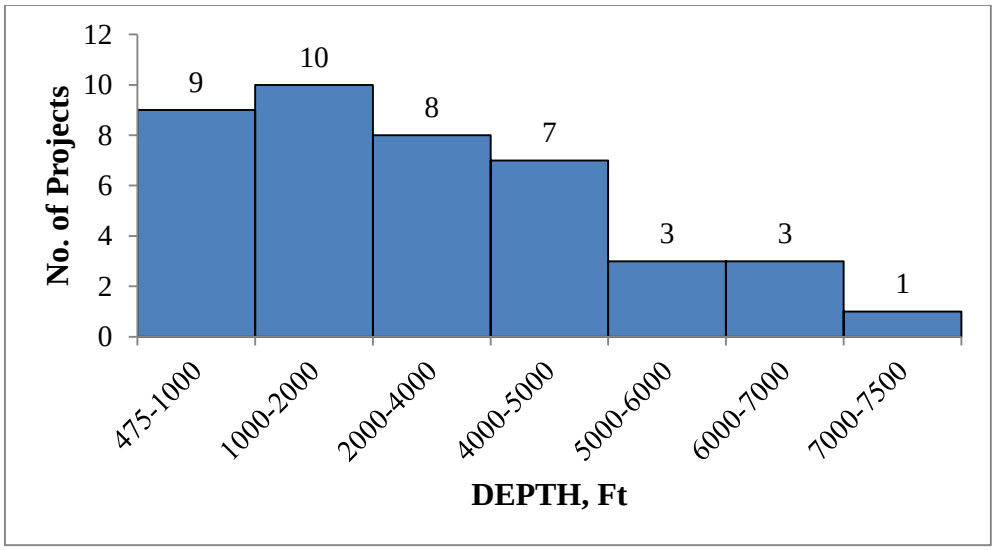

Figure 3.14 Reservoir depth range of the dataset

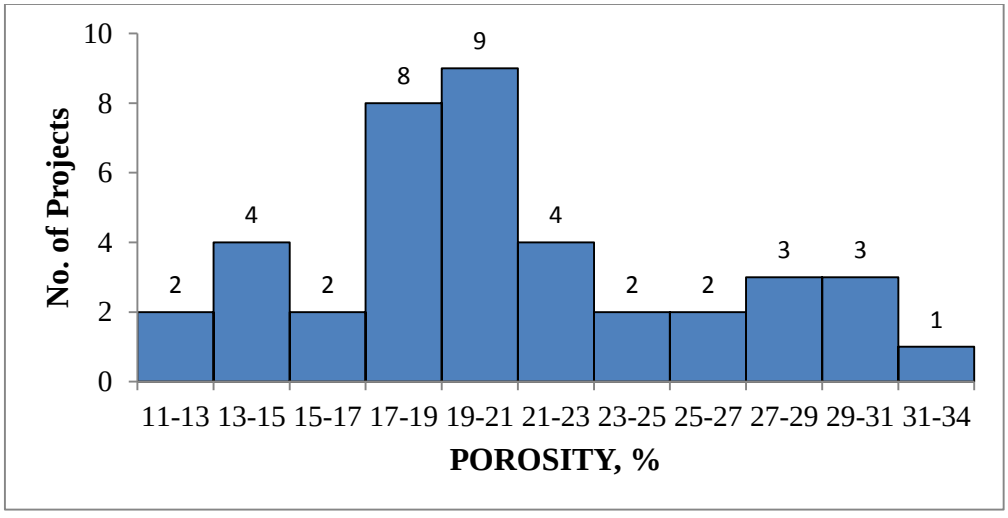

Figure 3.15 Porosity range of the dataset

Figure 3.15 shows a histogram of reservoir porosity of the dataset for 40 field projects. The highest frequency porosity lies between 17 to 23%. Approximately 52% of the porosity values lie in this range. The maximum porosity value of 34% is shown between 31-34%.

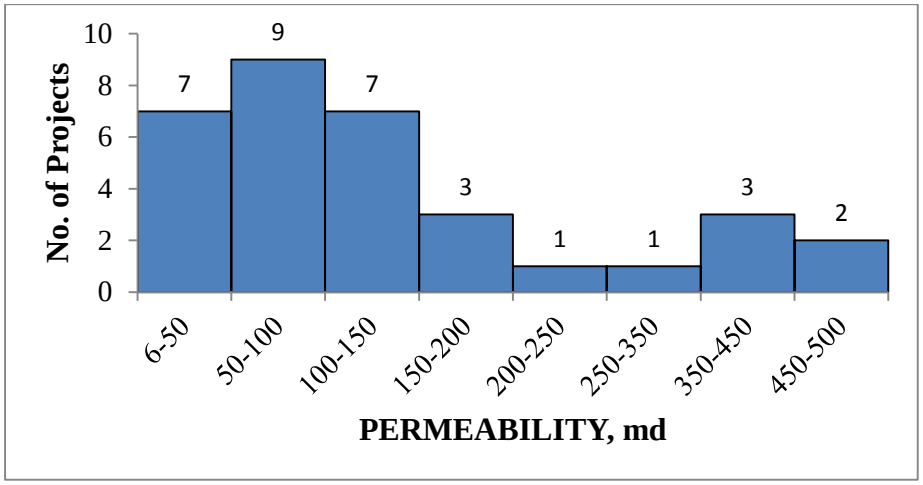

Figure 3.16 Reservoir permeability range of the dataset

Figure 3.16 shows a histogram of reservoir permeability of sandstone formations. The permeability range is across 35 field projects. 7 permeability values of reading above 1000md were excluded as special cases. These fields had high values as they consisted of unconsolidated formation. Majority of the permeability values lie in the range of 6-150md. Approximately 71% of the permeability values lie between 10-150md. The minimum value of 6md was of the reservoir in Bothamsall field of the United Kingdom.

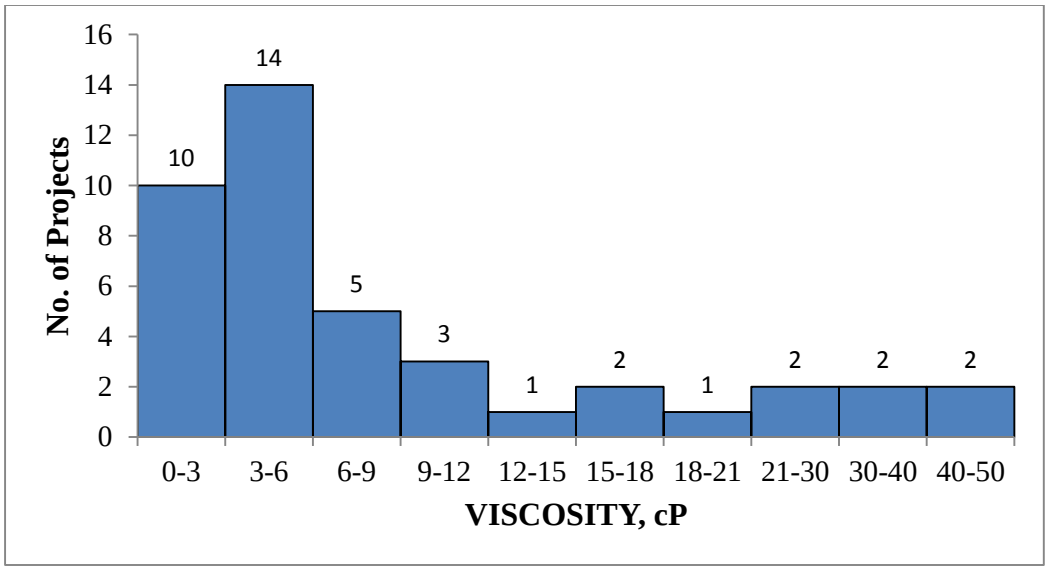

Figure 3.17 Oil viscosity range of the dataset

Figure 3.17 shows a histogram of oil viscosity of the dataset across 42 field projects. The figure is shows high frequency to the left. The highest peak is for the range of 3-6 cP. Approximately, 72% of the viscosity values are in the 0-12 cP range. Few oil viscosity values ranged from 21-50 cP, with the maximum value of 50 cP. The values of 45 and 50 cP were observed for the field projects conducted in China.

Figure 3.18 shows a histogram of oil gravity °API of the dataset across 39 field projects. It can be inferred from the histogram that most of the values lie in the range of 28-42°API suggesting that Surfactant-Polymer flooding projects are generally applied in reservoirs containing light oil. The distribution, as can be seen is skewed to the left. Approximately, 72% of the oil gravity values lie between the 28-41° API range.

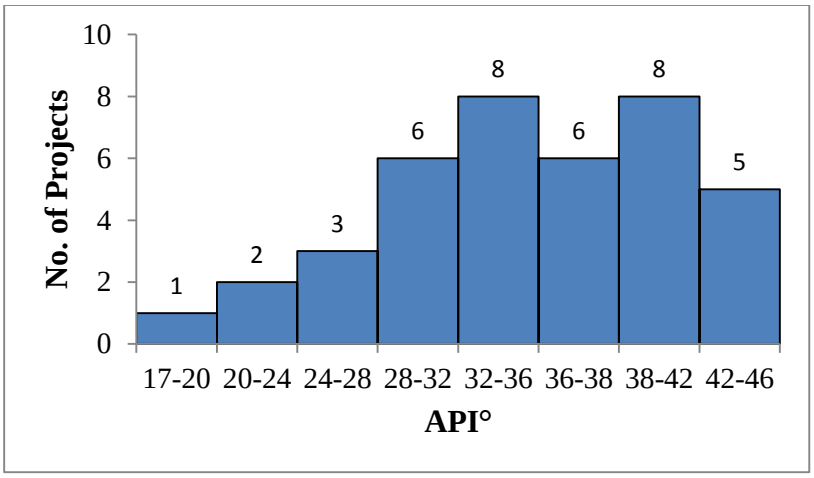

Figure 3.18 Oil gravity range of the dataset

Figure 3.19 shows the histogram for oil saturation (start). The dataset for oil saturation (start) comprise of 35 field projects. The highest peak in the distribution lies between 30% and 35%. The diagram is skewed to the right. Also, 66% of the data values fall between 30 and 40%. This is usually the residual oil saturation at the end of water-flooding.

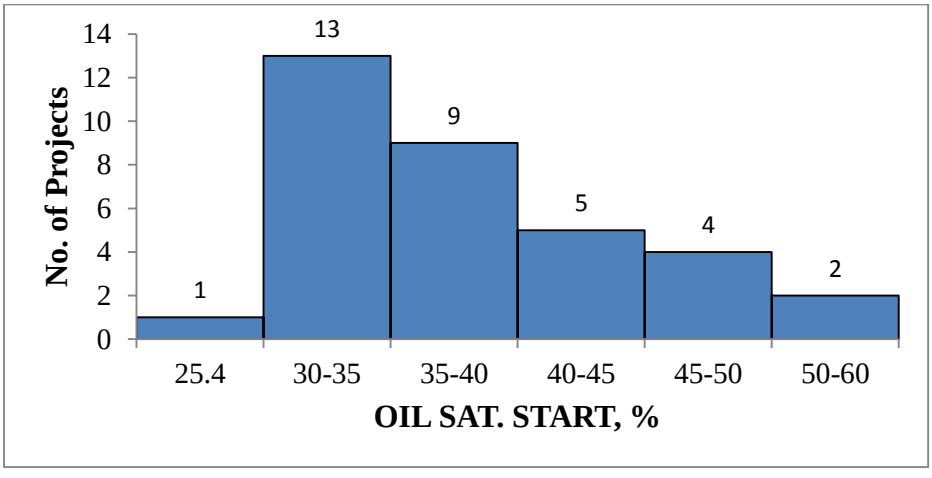

Figure 3.19 Oil saturation (start) range of the dataset

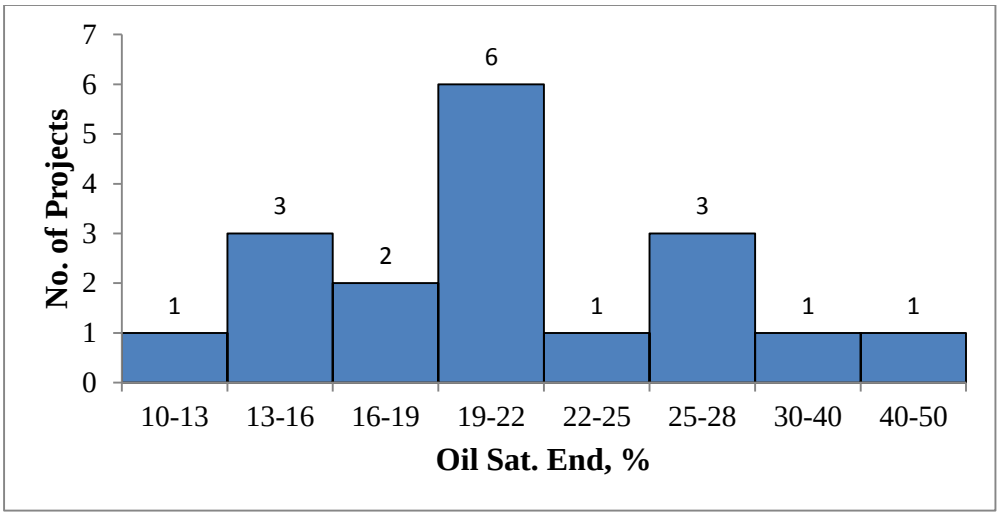

Figure 3.20 Oil saturation (end) distribution of the dataset

Figure 3.20 shows the oil saturation (end) distribution of the dataset across 16 data points ranging from 10 to 28%. The highest oil saturation (end) frequency occurs between 19 and 22%. Approximately, 69% of the oil saturation (end) values fall between 13 and 22% range.

Box-plot: The box-plots as described earlier were used to detect the special cases and inconsistent data in the dataset. However, they were also used to display the ranges and summarize the dataset for each parameter. Figure 3.21 shows the box-plots for different parameters for surfactant-polymer chemical flooding process. Data value ranges were provided for each parameter (minimum and maximum value) after omitting the data analyses. The minimum and maximum value range was illustrated by the distance between the opposite end of the whiskers. Additionally, the box-plots also show information such as mean and median of each parameter.

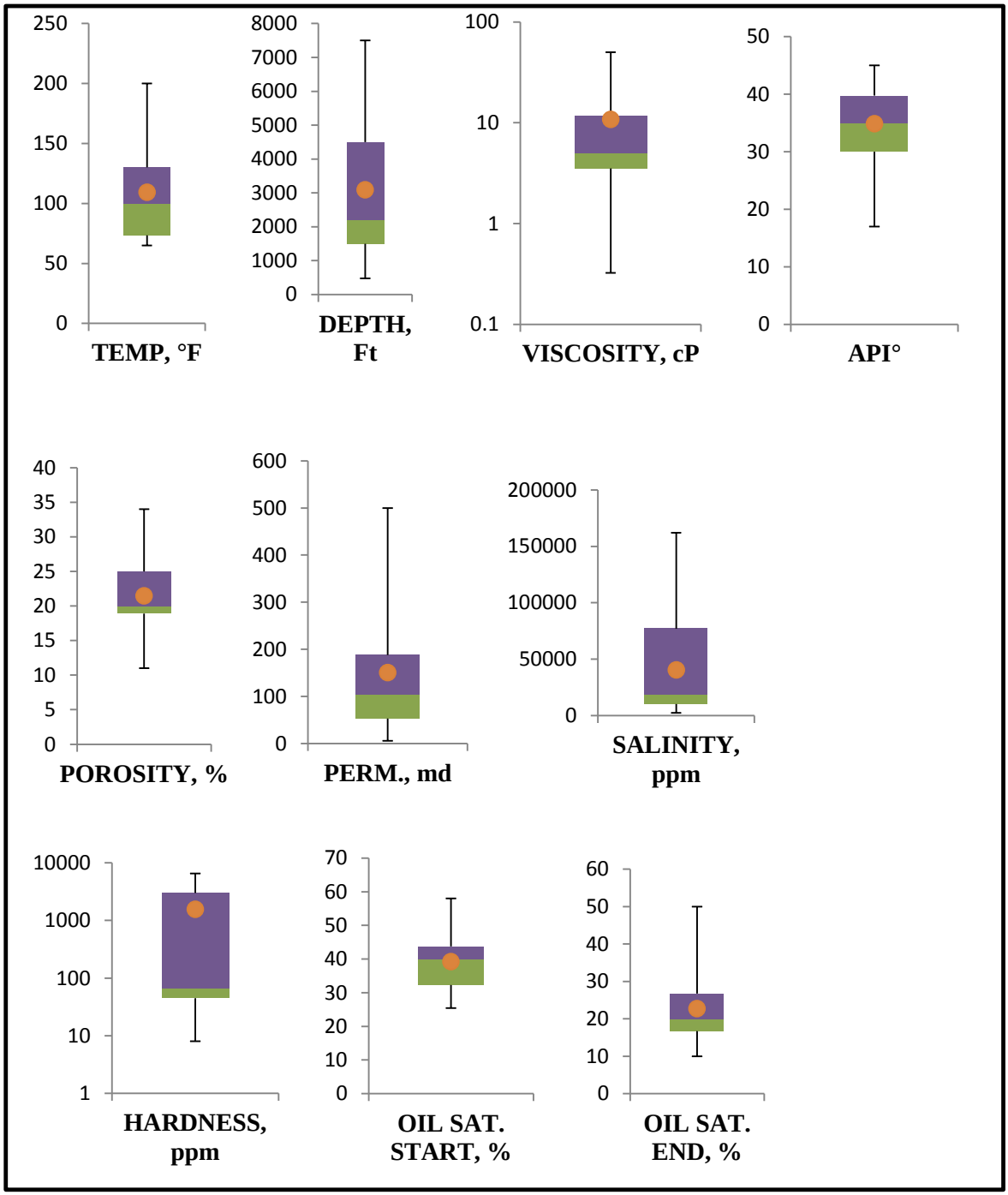

Figure 3.21 Left- Right-Box plots of Reservoir temperature, Depth, Oil viscosity, Oil gravity, Reservoir porosity & permeability, Brine Salinity & Hardness, Oil saturation start & end

Figure 3.21 shows box-plots of all the important parameters of the field projects. The box-plots show the mean and median values of all the parameters along with the minimum and maximum values denoted by the whiskers.

3.2 LABORATORY DATA

Most of the screening criteria work which has been published so far consists of field projects and pilot projects for various EOR processes. However, continuous laboratory research is been carried out to improve EOR processes. A good amount of research is also carried out in Surfactant-polymer chemical flooding process.

A dataset of laboratory work was established comprising of experiments for Surfactant-polymer flooding method. The dataset source comprised of information obtained from various publications in the SPE literature of onepetro. The dataset includes different experiments published to study properties and efficiency of surfactant-polymer flooding. All the injection experiments were carried out in various cores to study the efficiency of the flood for oil recovery.

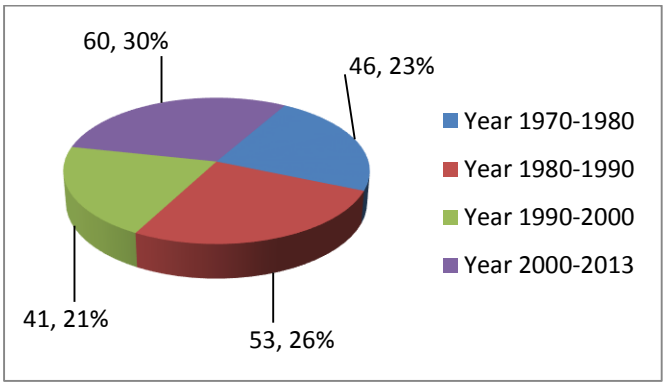

Figure 3.22 Laboratory surfactant-polymer flooding experiments from 1970-2013

Figure 3.22 shows the distribution of laboratory work on surfactant-polymer flooding carried out over the years. It shows the number of experiments which were conducted from 1970-2013. The turn of 20th century saw the most number of experiments carried out to check the efficiency of SP flooding. Sixty experiments in our dataset were executed in the years 2000 to 2013. Also, 99 experiments took place from 1970 to 1990, which is EOR boom period.

Figure 3.23 shows the different surfactants which were used in the experiments to establish a surfactant slug. Including the 4 basic surfactants such as Anionic, Non-ionic, Cationic, and Zwitterionic surfactants, there emerged a class of Bio-surfactants, which are generated through microbes and bacteria. The pie-chart (figure 3.22), illustrates the percentage and number of experiments conducted in each category. Zwitterionic dataset was the smallest as this class of surfactants was only recently proposed for research.

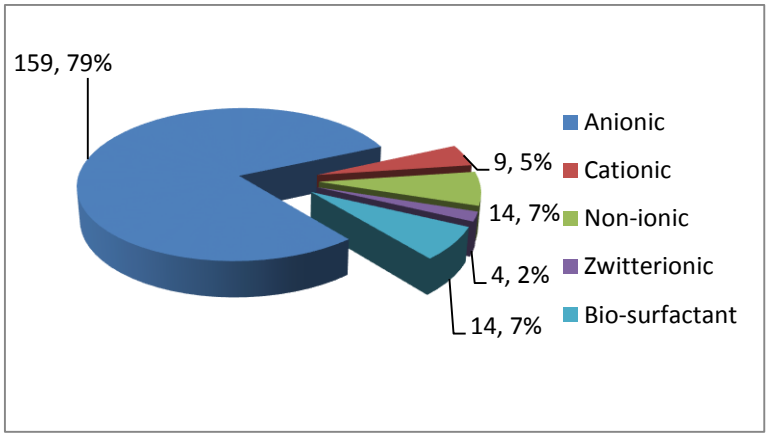

Figure 3.23 Distribution of types of Surfactants used in laboratory dataset

Conventional, anionic surfactants were used in most of the experiments, resulting in the biggest dataset. Over 79% of 200 experiments used anionic surfactants to study their effect on oil recovery.

Figure 3.24 depicts the type of polymers used in the dataset. It shows the percentage and number of 4 different types of polymer viz. Hydrolyzed polyacrylamide, xanthan gum, bio-polymer and associating polymer used in the experiments. HPAM was the most common polymer used; while only a few experiments were conducted using a new emerging class of Associating polymer.

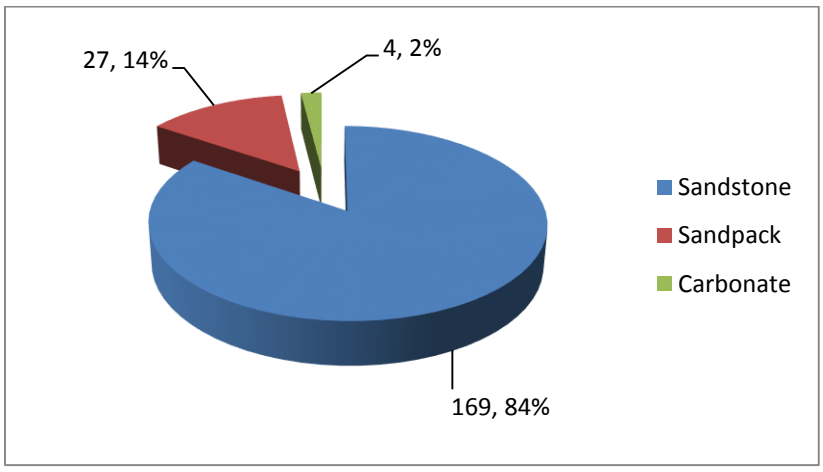

Figure 3.24 Types of Cores used in the Laboratory dataset

Sandstone cores, sandpacks and carbonate cores were the 3 major types of cores used in the tests. More than 80% of the tests were conducted in the sandstone cores including Berea, Bentheimer, Briarhill and Reservoir cores. Few tests (14%) were

conducted in sandpacks, while even fewer were conducted in non-fractured carbonate cores.

3.2.1. Data Analysis. Data analysis included representing the data with the help of box-plots, histograms and cross plots.

Cross plots were used to analyze the related parameters for example, core porosity vs. core permeability, the Oil viscosity vs. Oil gravity, Oil recovery (% of residual oil saturation after water-flooding) vs. Surfactant slug concentration and oil viscosity.

In descriptive statistics, a box-plot is a statistical way to graphically describe a group of numerical data by their quartiles. The box-plot used in this study divides the set of data into 6 parts as follows.

1. The lowest value (minimum)
2. The highest value (maximum)
3. The mean value (Average data value)
4. The first quartile (25^{th} percentile)
5. The second quartile (50^{th} percentile)
6. The third quartile (75^{th} percentile)

Figure 3.25 shows a schematic of a box-plot used to display the data. Histograms, as previously used to depict the range of different reservoir and oil parameters for field projects, were also used to observe the range of different laboratory parameters.

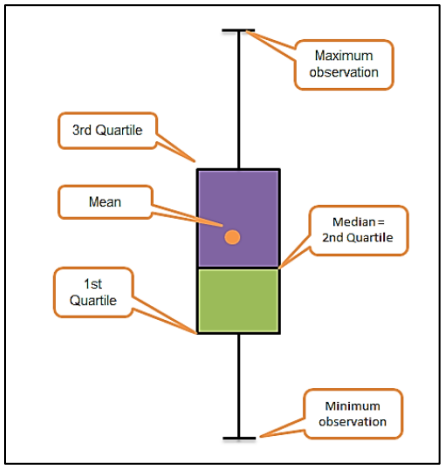

Figure 3.25 Schematic of a box-plot

Figure 3.26 shows a cross-plot of oil viscosity vs. oil gravity of the crude oil used in different tests. One test, as is evident by the diagram showed oil viscosity of 376 cP and gravity of 16.5°F. A test using such heavy oil was conducted to study the efficiency of the surfactant-polymer flooding process in heavy oil reservoirs of Canada.

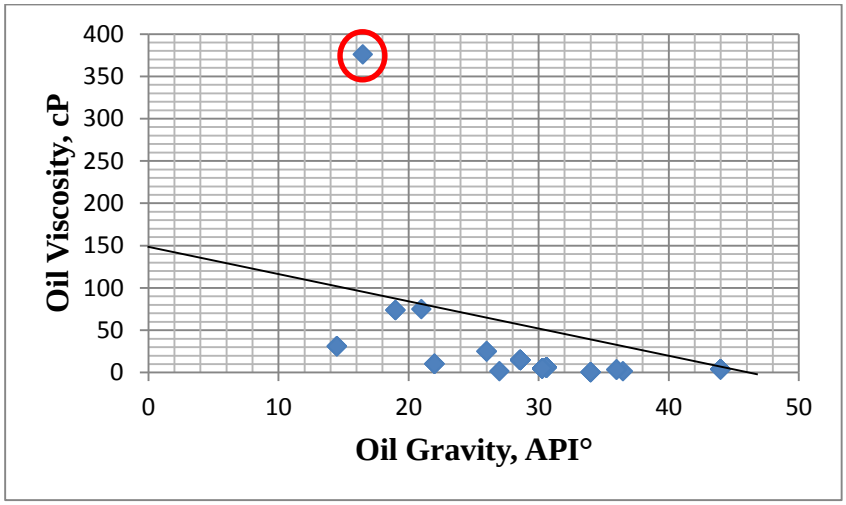

Figure 3.26 Cross plot of Oil viscosity vs. oil gravity

It shows a very few data-points as some experiments used crude oil with same oil viscosity and oil gravity. Also, many experiments only mentioned the oil viscosity and not the oil gravity °API.

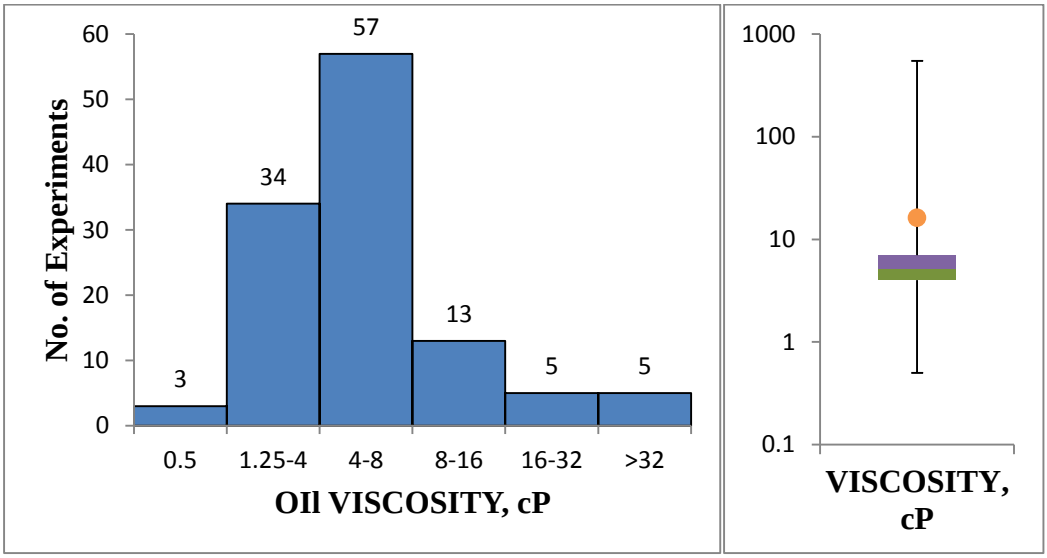

Figure 3.27 Oil viscosity histogram (left) and oil viscosity box-plot (right)

Figure 3.27 depicts the histogram and box-plot of oil viscosity values used in the experiments. The lowest oil viscosity value was of 0.5cP while the highest oil viscosity value was of 550cP, which is denoted by the >32 bar in the histogram. It can be inferred from such high oil viscosities that the surfactant-polymer flooding is being tested for recovery efficiency of heavy crude oil, to increase the application range of the method.

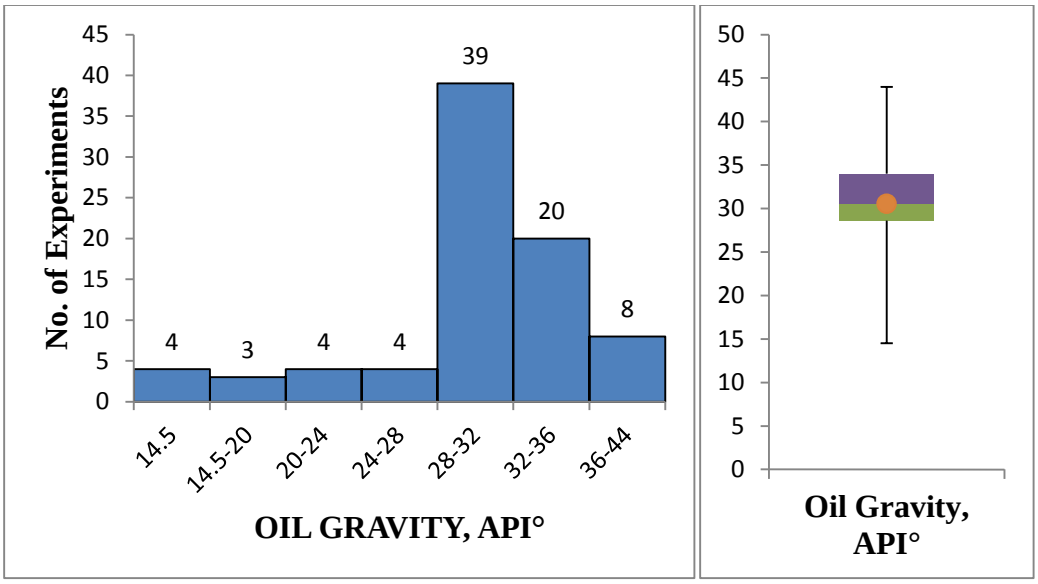

Figure 3.28 Oil Gravity histogram (left) and oil gravity box-plot (right)

Figure 3.28 shows the range of oil gravity °API with the help of histogram and the box-plot. The minimum value was 14.5° API and further the low values observed were between the values of 14.5 to 20°API. Such low values were observed for the experiments in which heavy crude oil with high viscosity were used. The new proposed class of zwitterionic (amphoteric) surfactants was tested for recovery in heavy oil reservoirs. A few experiments were conducted for a crude oil with viscosity of 75cP. An Alkoxy Carboxylate surfactant with large hydrophobic tail was used to check its stability in the presence of high viscosity oil. Oil recovery results for these experiments showed promising results.

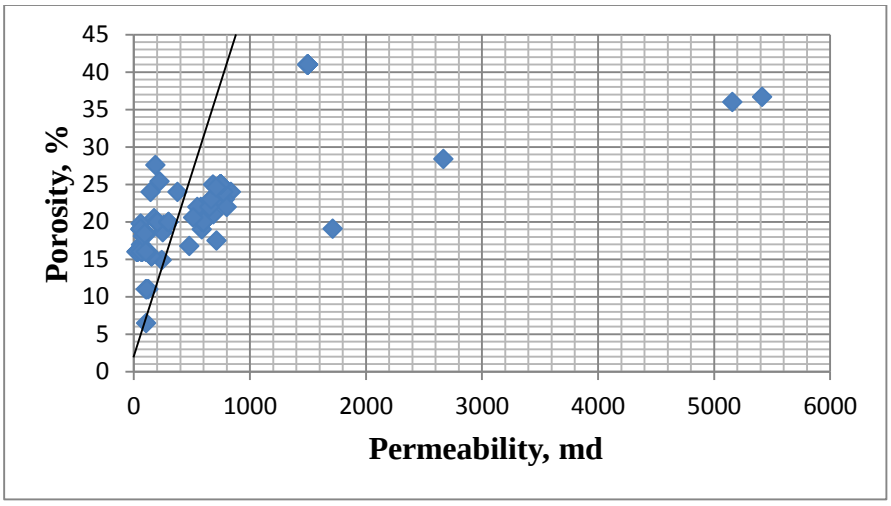

Figure 3.29 Cross-plot of core permeability vs. core porosity

Figure 3.29 shows a cross-plot of core permeability vs. core porosity. The data-points show a consistent relationship between the porosity and permeability values. However, five peremeability values lie on the higher side, over 1000md. These high permeability values were observed for sandpacks. Sandpacks are the loosely packed grains of sand which are generally used to observe the behaviour of the chemical slug in the formation and its interaction when it comes in contact with the crude oil. The minimum value observed in the cross-plot was of 106 md of reservoir core.

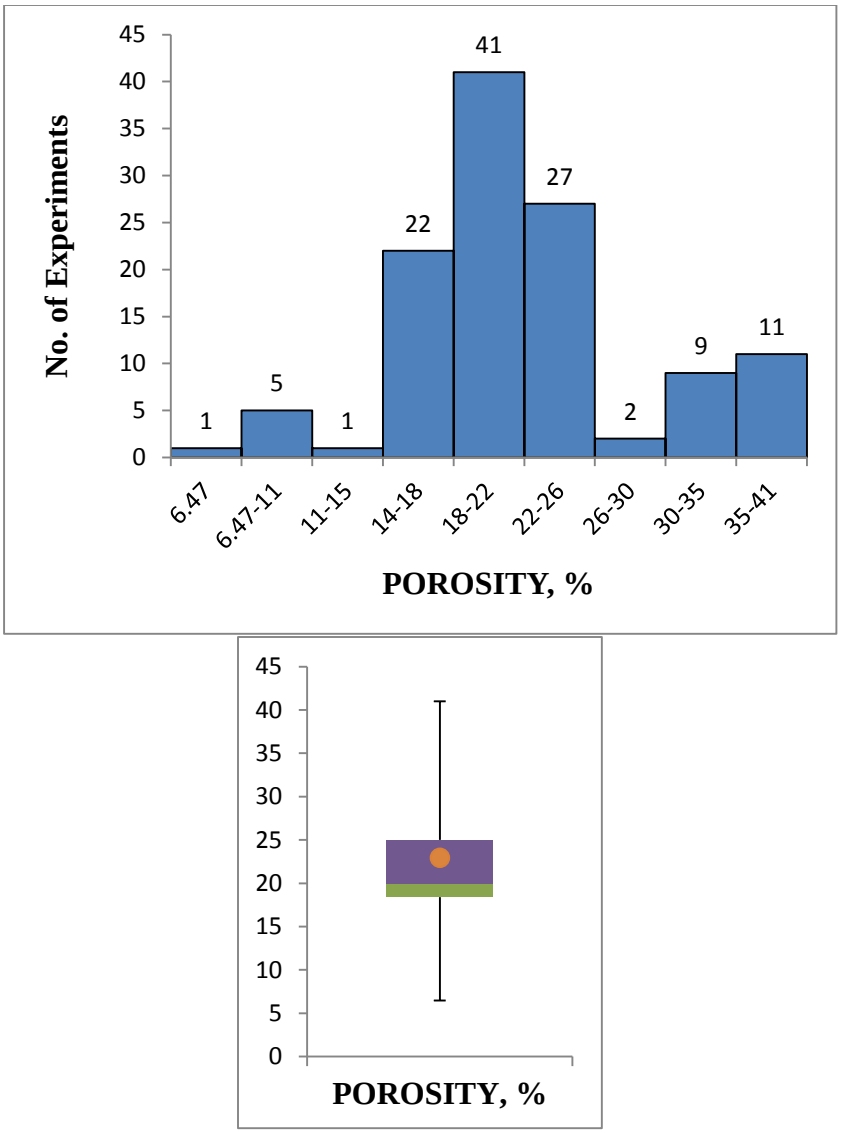

Figure 3.30 Core porosity histogram (above) and core porosity box-plot (below)

Figure 3.30 represents the range of core porosity with the help of a histogram and a boxplot. As we study the diagram, it can be inferred that the highest peak of core porosities was observed in the range of 18 to 22. Approximately, 76 percent of the porosity values lie between 14-26%. The lowest value of porosity observed was of

6.47%. This value was the porosity value measured for a reservoir core. The porosity box-plot shows a spread of porosity values between 6.47 to 41%, with the mean at 23.9%.

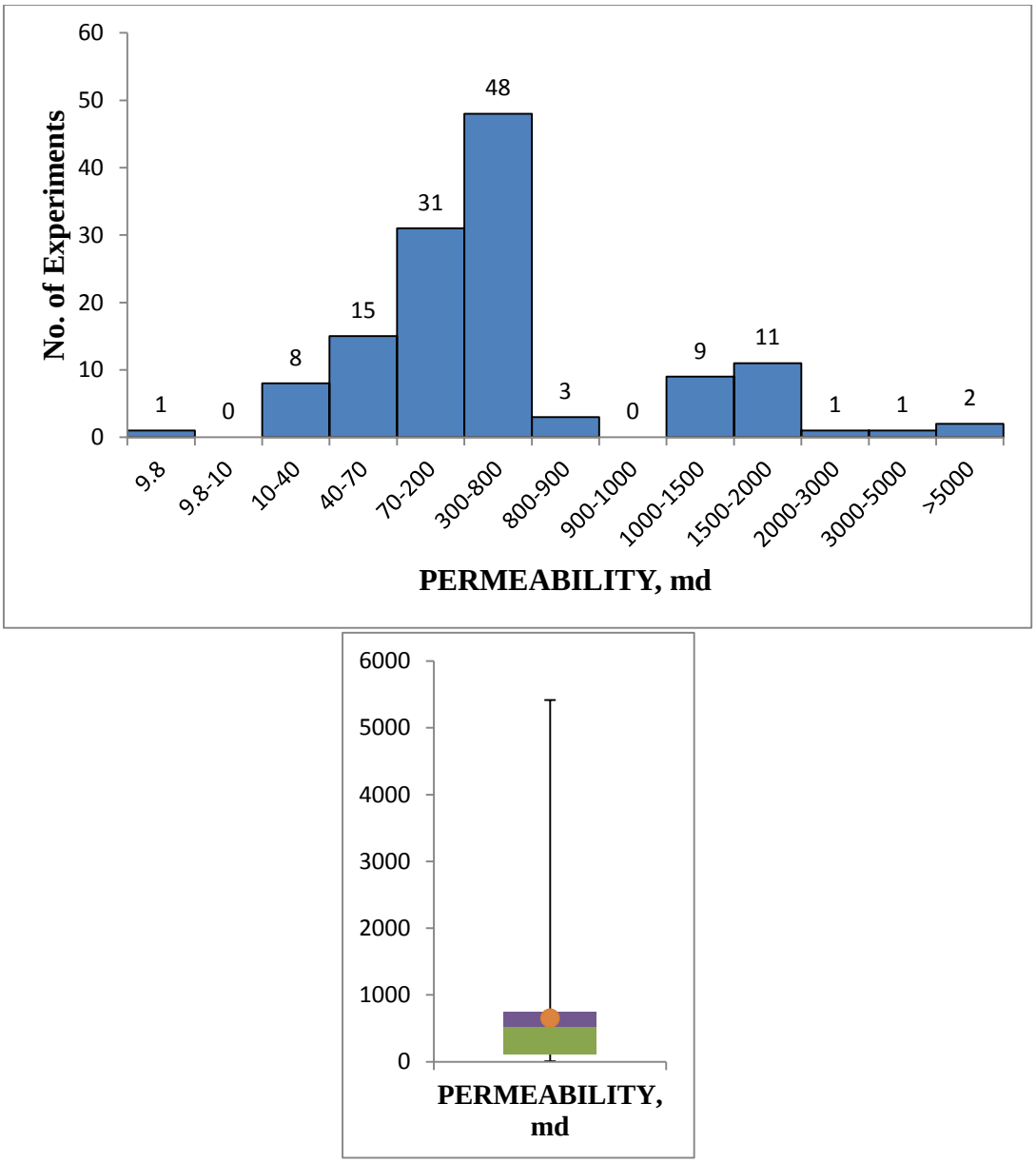

Figure 3.31 permeability histogram (above) and permeability box-plot (below)

Figure 3.31 shows the distribution of permeability values for the different cores used in the tests. It can be concluded from the histogram and permeability box-plot that the permeability values are spread over a wide range from 9.8md to over 5000md. Majority of the values in the dataset lie between 70 and 800. However, the permeability values vary significantly from one core to other core, for instance, one of the reservoir core permeability was 2668md, while most of the reservoir cores had permeability values of less than 1000md. Also, the high permeability values (greater than 1000md) are observed for sandpacks and few Bentheimer cores.

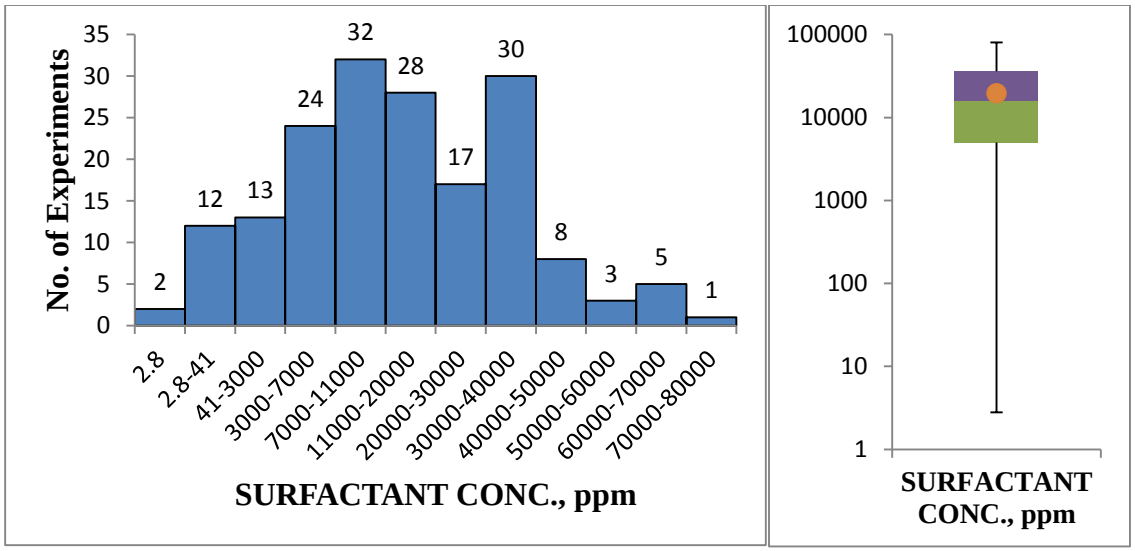

Figure 3.32 Surfactant slug concentration histogram (left) and box-plot (right)

Figure 3.32 gives the range for surfactant slug concentration used in the tests in

our dataset. Majority of the values lie in the range of 5000 to 40,000 parts per million (ppm). Approximately 77% of the 175 surfactant concentration values lie in the aforementioned range. It can also be inferred that a few values are as low as 2.8ppm. Concentrations of bio-surfactants used in a few experiments had a range of 2.8ppm to 41ppm. The box-plot of surfactant slug concentration shows a mean of 20,355.6ppm. High concentration of surfactant slug (over 50,000ppm) in the subset was observed for tests which used surfactant blend of petroleum sulfonate and non-ionic surfactant. The concentration measured was a combination of these surfactants.

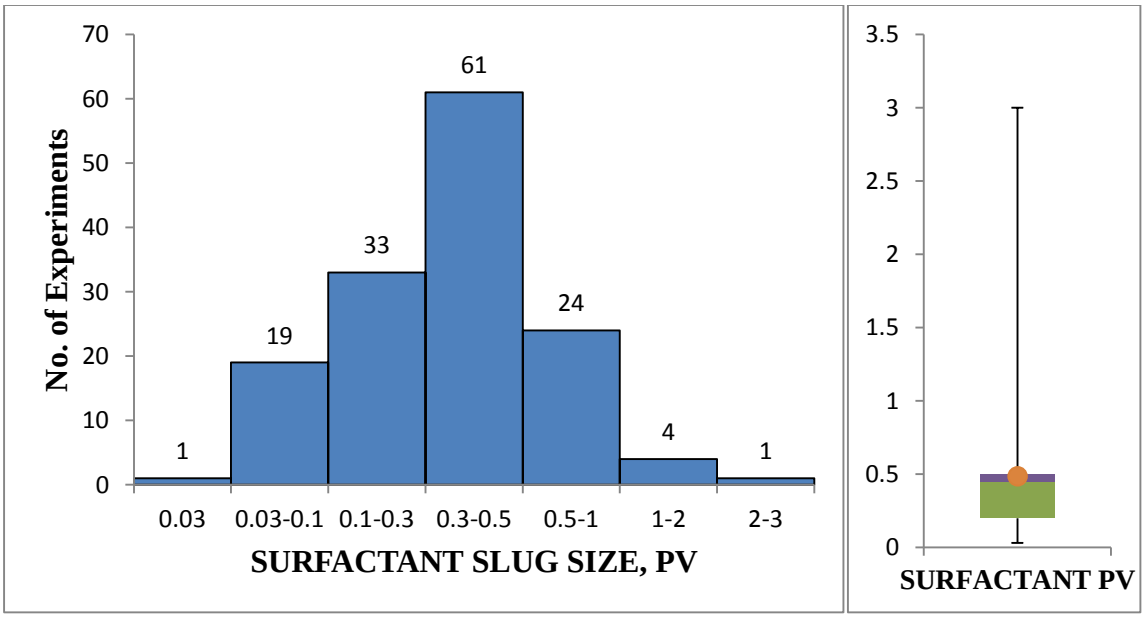

Figure 3.33 Surfactant slug size histogram (left) and box-plot (right)

Figure 3.33 depicts the range of surfactant slug size in terms of pore volume injected. The surfactant slug size of the subset ranged from 0.03 to 3. As can be inferred from the plots, majority of the values lie between 0.041 and 0.9. The surfactant slug size over 1PV were used in bio-surfactant tests.

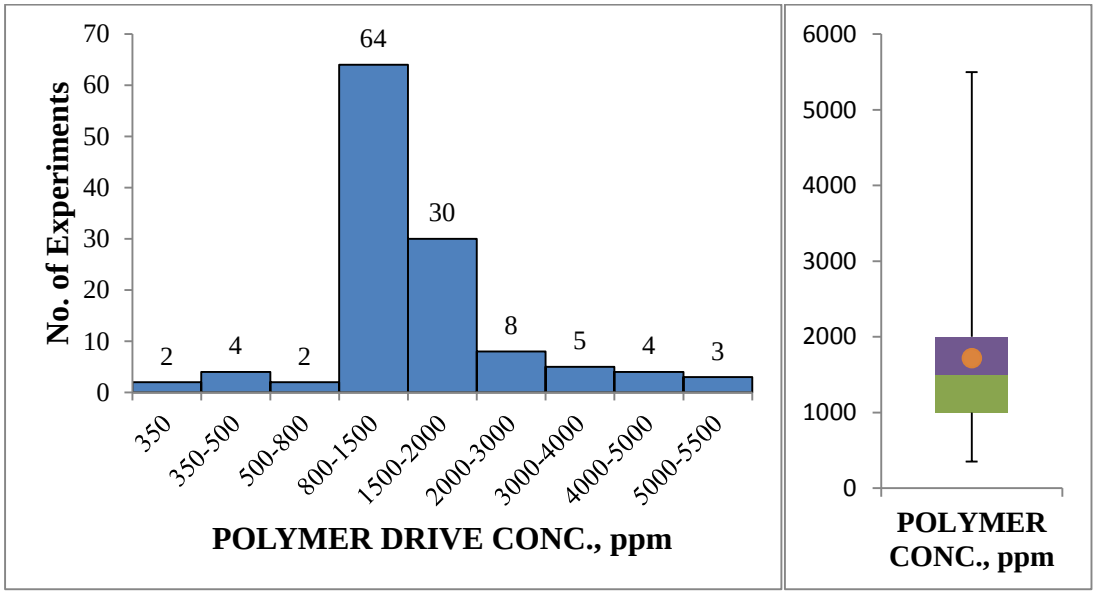

Figure 3.34 Polymer drive concentration histogram (left) and box-plot right

Figure 3.34 illustrates the range of polymer drive concentration (parts per million) with the help of a histogram and box plot. Majority of the tests were conducted with polymer concentration of 800 to 2000 ppm. 74 of the 121 values in the subset lie in this

range. Few values in the dataset were high in the range of 4000-5000ppm. These were bio-polymer concentrations.

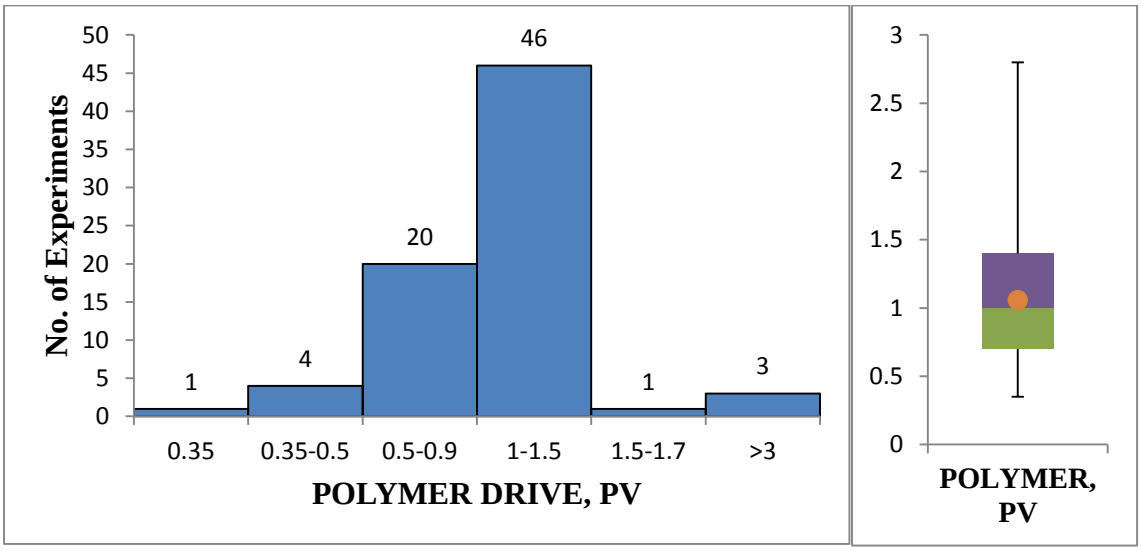

Figure 3.35 Polymer drive slug size histogram (left) and box-plot (right)

Figure 3.35 gives the range of polymer drive slug size in terms of total pore volume injected. The minimum value observed in the dataset was 0.35 PV while the maximum value observed was 2.8 PV. Majority of the values in this subset were in the range of 0.5PV to 1.5 PV. The maximum slug size of 2.8 PV was observed for a test conducted in reservoir sandstone core to achieve a favourable mobility ratio.

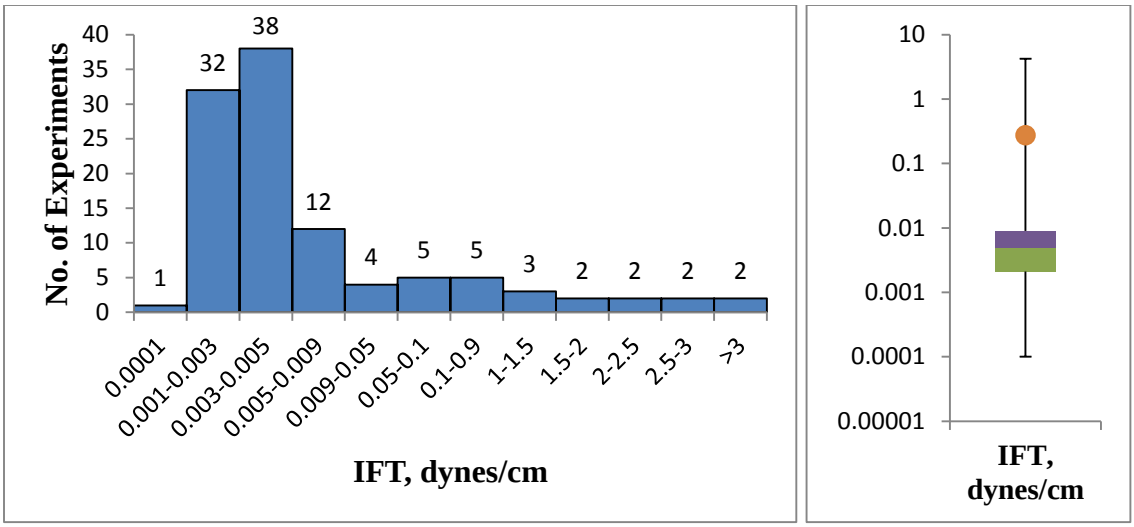

Figure 3.36 IFT between oil-water-surfactant system histogram (left) and box-plot (right)

Figure 3.36 shows the interfacial tension (IFT) values between oil-surfactant-water system. It can be inferred that the IFT values in the dataset had a wide spread from 0.0001 dynes/cm to 4.2 dynes/cm. The higher IFT values were observed for the oil-surfactant-water system in which bio-surfactants were used. Also, as can be interpreted from the IFT box-plot, the mean of the subset 0.274 dynes/cm because of these high values ranging from 1 dynes/cm to 4.2 dynes/cm.

Figure 3.37 shows the range of dynamic adsorption of anioinic surfactants on sandstone adsorbent. The adsorption was measured in terms of milligrams of surfactant adsorbed per gram of adsorbent. Majority of the adsorption values ranged from 0.1mg/g to 0.6mg/g. Few of the surfactants had high surfactant adsorption, ranging from 1 mg/g to 4.2 mg/g. These were observed for reservoir sandstone cores, where adsorption increases due to reservoir heterogenity.

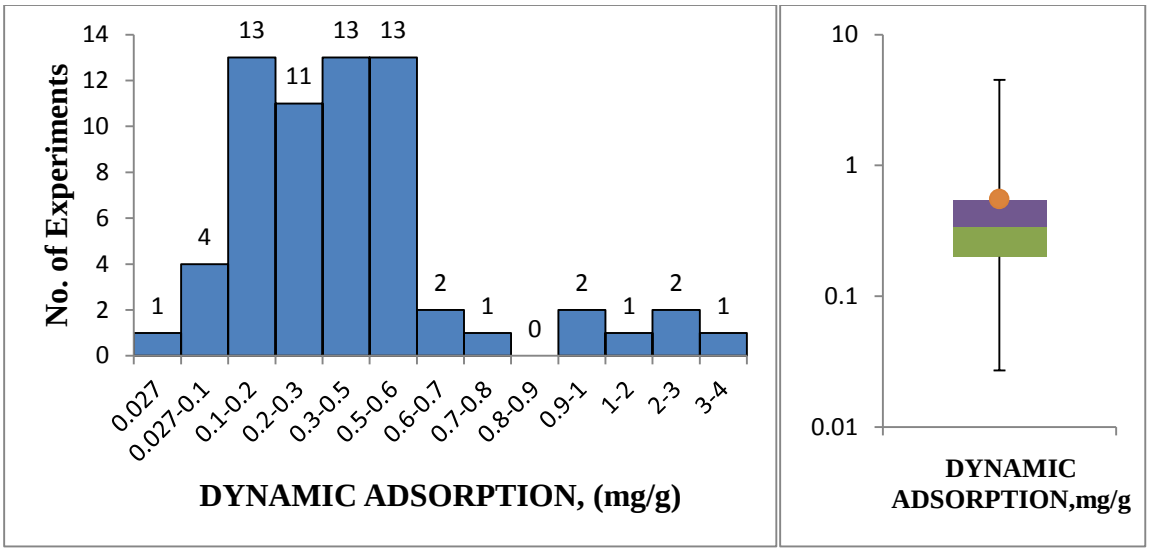

Figure 3.37 Dynamic adsorption histogram (left) and box-plot (right)

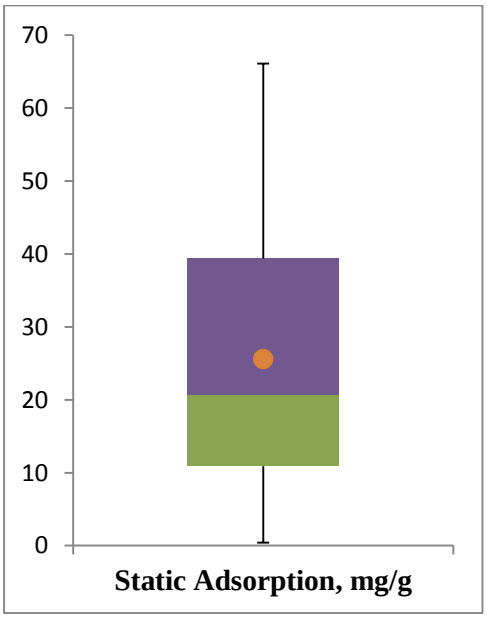

Figure 3.38 Static adsorption box-plot

Figure 3.38 shows the range of static adsorption of anionic surfactants on kaolinite adsorbent. It can be inferred from the box-plot that the adsorption ranges from 0.4 mg/g to as high as 66.1 mg/g. When compared with dynamic adsorption, static adsorption has higher values. This can be attributed to kaolinite adsorbent used in the static adsorption experiments. Since clay has higher surface area than sandstone, more surfactant is adsorbed on it.

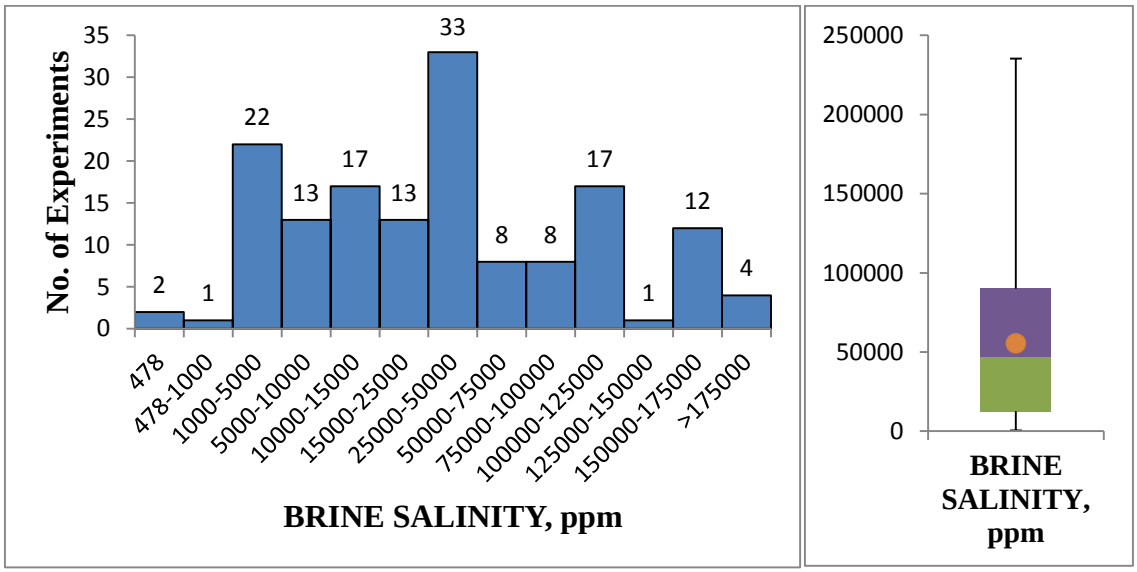

Figure 3.39 Brine salinity histogram (right) and box-plot (left)

Figure 3.39 shows the brine salinity distribution with the help of a histogram and a box-plot. It can be inferred from the graph that the minimum and maximum values for

brine salinity was 478ppm and 235,000ppm respectively. Such high brine salinity values were observed for surfactants which were tested for harsh reservoir conditions of salinity and hardness.

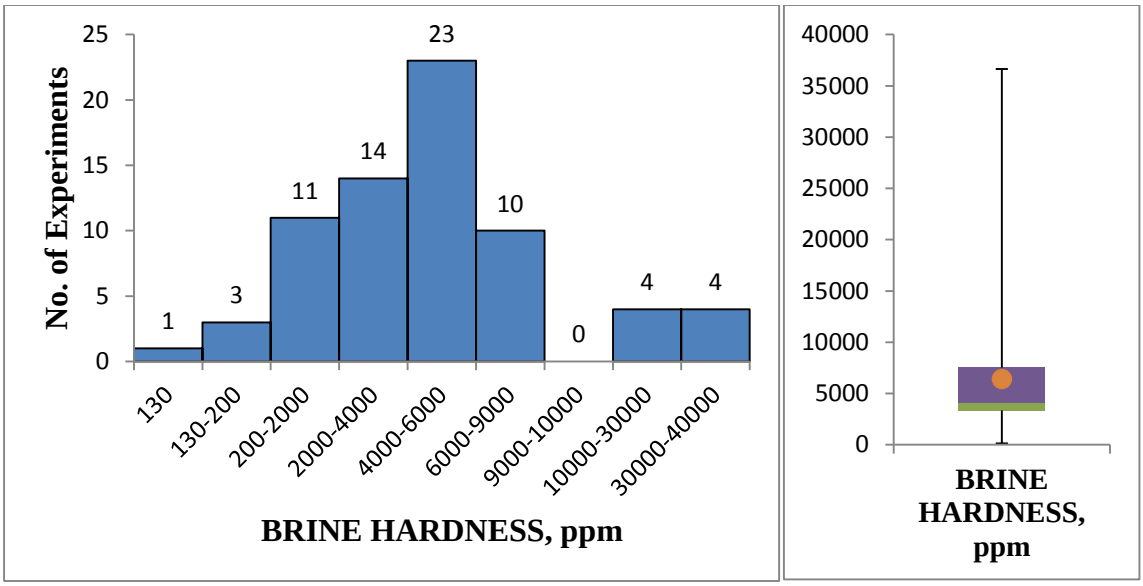

Figure 3.40 Brine hardness histogram (right) and box plot (left)

Figure 3.40 illustrates the distribution of brine hardness subset. It can be inferred that the brine hardness values had a wide spread from 130ppm to as high as 40,000ppm. The high hardness values were observed in some tests conducted to check surfactant stability in harsher reservoir conditions conataining hard brines.

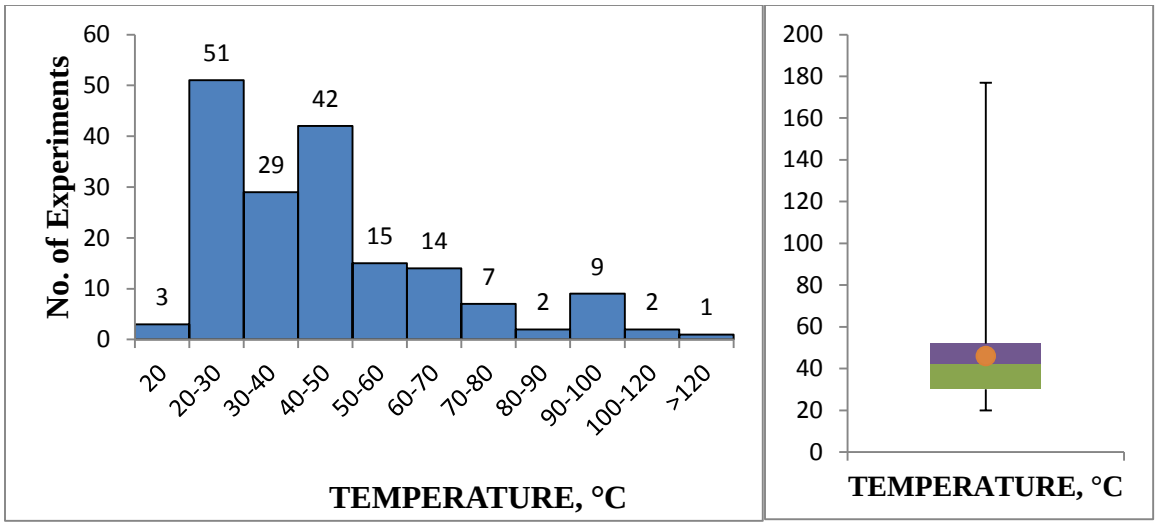

Figure 3.41 Temperature histogram (left) and box plot (right)

Figure 3.41 shows the range of temperatures under which the experiments were conducted. The values show a wide range of spread between 20°C to 177°C. It can be inferred from the figure that few experiments were conducted under high temperatures for instance; one test was conducted at a temperature of 177°C (350°F) to test the stability of surfactant (akyl aryl sulfonate) at such high temperature.

Figure 3.42 illustrates a cross plot of Surfactant slug concentration (parts per million) vs. the tertiary oil recovery of fraction of oil in place after waterflooding for all the tests performed. The oil recovery, as can be concluded varies significantly from core to core. This prominent difference between oil recoveries for the cores can be attributed to the type of cores being used to check the efficiency of the surfactant-polymer flooding. Berea sandstone cores, Briarhill sandstone cores, Bentheimer sandstone cores were used in most of the tests. These standard cores are more homogenous than the reservoir cores.

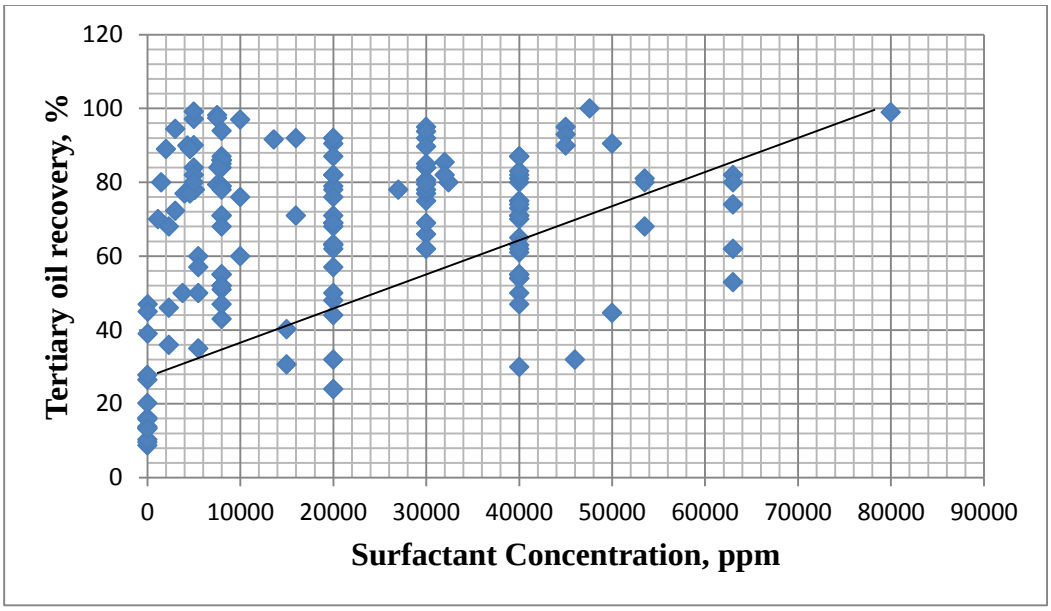

Figure 3.42 Cross-plot of surfactant concentration vs. tertiary oil recovery (after waterflooding)

Low residual oil recovery in the reservoir cores was attributed to the heterogeneity of the rock, which affected the stability of the chemical slug which resulted in higher surfactant retention (adsorption) and affected the micro-emulsion phase, which in turn affected the size of the oil bank formed. Surfactant slug concentration injected in the cores also affected the tertiary oil recovery. For example, in tests where low concentration of bio-surfactants was used, the oil recovery was poor. However, when high concentration of surfactants (47,600 ppm) was injected in a core, all of the residual oil was recovered as indicated by the cross-plot above. Figure 3.43 shows the range of percentage of tertiary oil recovery after waterflooding. The values of the subset had a wide spread between 19.5% to 100% tertiary oil recovery. Most of the low oil recoveries

were observed for reservoir sandstone cores, while higher tertiary oil recoveries were measured for more homogenous Berea sandstones, Briarhill sandstones.

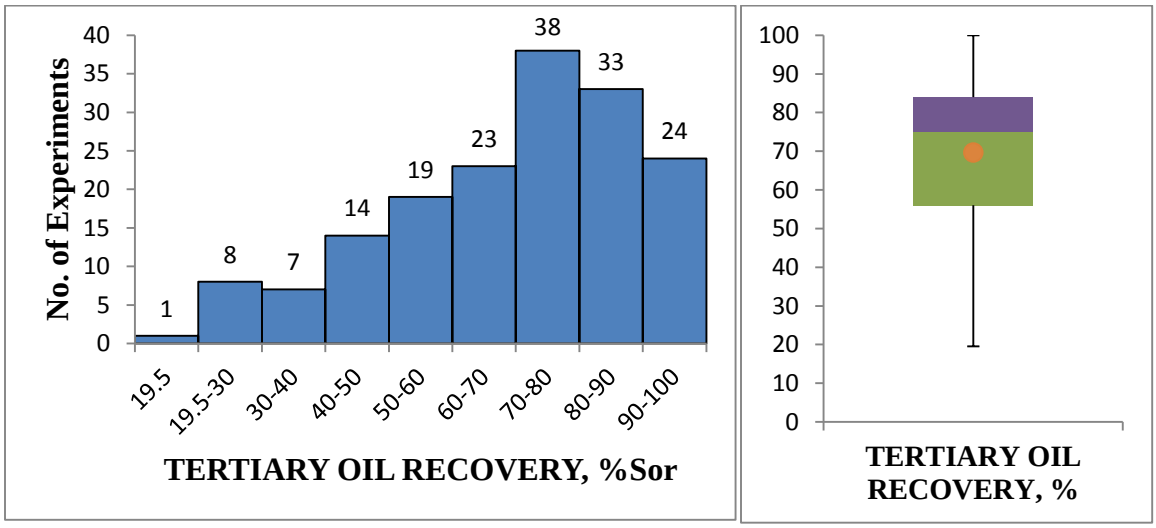

Figure 3.43 Tertiary oil recovery histogram (right) and box-plot (left)

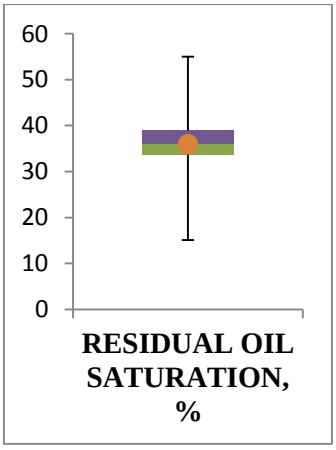

Figure 3.44 Residual oil saturation box-plot

4. SUMMARY AND CONCLUSION

After, detailed representation of both field and laboratory datasets, the established summary was presented in the following section. Summary for field projects was compared to the previous work. Eventually, a comparison was made between the established ranges of laboratory and field datasets.

4.1 SUMMARIZING THE FIELD DATASET

Table 4.2 below gives the range for surfactant-polymer flooding on the basis of statistical analysis for a cleaned dataset. The summary includes all the parameters which eventually decide success or failure of a surfactant-polymer flooding project. The statistical parameters used to define the range were mean, median, standard deviation, minimum and maximum values.

The ranges for the parameters was eventually compared with the previous work and the differences were noted.

1. The concluded summary of oil gravity had a range from 17°API to 45°API. Brasear (1978), Carcaoana (1982) and Goodlett (1986) suggested a value greater than 25°API, while Taber (1997) suggested a value to be greater than 20°API. Aldasani and Bai gave a range of 22°API to 39°API, with and average value of 34.8°API.

2. Oil viscosity in the study has a range of 0.32cP to 50cP, while authors like Caracoana (1982), Peter H. (2984) and Goodlett (1986) suggested a value less than 30cP. On the other hand, Taber (1997) suggested a value of less than 35cP for oil viscosity. Aldasani and Bai concluded a range of 15.6 to 3 cP and a mean of 9.3cP.
3. Temperature range in the study was from 65°F to 200°F. Most of the authors suggested the value to be less than 200°F (Table 2.3), while Caracoana (1982) and Al-Bahar (2004) suggested a value less than 180°F and 158°F respectively. The temperature range differed from previous work conducted by Aldasani and Bai, as they concluded a range of 122-155°F with a mean of 138.5°F
4. Depth range was concluded to be between 475 ft to 7500ft which differed from the values of less than 7000ft and 9000ft suggested by Caracoana (1982) and Goodlett (1986) respectively.
5. Porosity value ranged from 11 to 34% in the study. However, Brashear (1978), Caracoana (1982) and Goodlett (1986) suggested a value of greater than 20%.
6. Permeability range was concluded to be between 6md and 500md. This range differed from the value proposed by most of the authors. Brashear (1978), Caracoana (1982), Peter H. (1984), Goodlett (1986), Taber (1997) and Al-Bahar (2004) suggested a value greater than 20md, 35md, 40md, 40md, 40md and 50md respectively.

Table 4.1 Summary of ranges for surfactant-polymer flooding for field dataset

Parameters	Mean	Median	Standard Deviation	Minimum	Maximum
Oil Gravity, °API	34.8	35	6.9	17	45
Oil Viscosity, cP	10.8	5	12.7	0.32	50
Temperature, °F	109.4	100	38.7	65	200
Depth, ft	3088	2200	2062	475	7500
Porosity, %	21.5	20	5.6	11	34
Permeability, md	150.9	103	135.64	6	500
Oil saturation start, %	39	40	8	25.4	58
Oil saturation end, %	22.7	20	9.6	10	50
Brine salinity, ppm	40,508	16,500	43,833	400	160,000
Brine hardness, ppm	1559	70	2166	13	6530

7. The minimum oil saturation start value in the dataset was 25.4%. This differed from the values suggested by Brashear (1978), Caracoana (1982), Goodlett (1986), Al-Bahar (2004), which were 25%, 30%, 30% and 35% respectively. Taber (1997) suggested a value of greater than 35%. Aldasani and Bai gave a higher range of 43.5 to 53.

8. The maximum salinity value in the dataset was 160,000ppm which differed from the maximum salinity values of 50,000ppm, 100,000, 140,000 and 50,000 proposed by Brashear, Peter H., Goodlett and Al-Bahar respectively.

The study on laboratory dataset showed a distinct difference than the field project dataset for surfactant-polymer flooding. The statistical data for different parameters have different ranges for laboratory dataset. Table 4.2 shows parameters like oil viscosity, oil gravity, temperature, porosity, permmeability, oil saturation start (residual oil saturation), tertiary oil recovery by surfactant-ploymer flooding, surfactant concentration, brine salinity, IFT and adsorption. IFT, surfactant adsorption and surfactant concentration were 3 parameters studied for laboratory dataset. A comparison between the field project dataset and laboratory dataset follows.

1. The obvious difference between maximum oil viscosities of field maximum (50cP) and laboratory criteria (550cP) was due to the use of new emerging visco-elastic surfactants used for recovery of heavy oil. Laboratory dataset contained an experiment which was tested for recovery of oil of viscosity 376cP. A new class of surfactants called Zwitterionic (amphoteric) surfactant was used in this experiment. Both the experiments were successful in terms of tertiary oil recovery.

Table 4.2 Summary of ranges for surfactant-polymer flooding for Lab. dataset

Parameters	Mean	Median	Standard Deviation	Minimum	Maximum
Oil Gravity, °API	30.5	30.6	6.6	14.5	44
Oil Viscosity, cP	16.3	5.2	61.4	0.5	550
Temperature, °C	46	42	23.3	20	177
Porosity, %	22.9	20	7.8	6.47	41
Permeability, md	657	529.5	845	9.8	5415
Oil Saturation (Start)	35.8	36	5.9	15.1	55
Oil Saturation (end)	12.5	11.45	8.3	0.5	38
Surfactant Concentration, ppm	20355.6	16000	17755	2.8	80000
Surfactant slug Size, PV	0.48	0.45	0.42	0.03	3
IFT, dynes/cm	0.274	0.005	0.79	0.0001	4.2
Adsorption, mg/g-Dynamic	0.55	0.34	0.78	0.027	4.51
Static	25.57	20.7	19.38	0.4	66.1
Brine Salinity, ppm	81154	50000	83294	478	350000
Brine Hardness, ppm	6398	4050	7989	130	36633
Polymer Drive Conc. ppm	1718	1500	1057	350	5500
Polymer Drive size, PV	1.05	1	0.46	0.35	2.8
Tertiary Oil Recovery, (%S_{or})	69.7	75	19.59	19.5	100

2. Maximum temperature value for field range was 185°F (85°C), which was

far less than the value of 177°C (351°F) observed in laboratory range. Experiment for high temperature resistant surfactant for steam assisted surfactant-polymer flooding was conducted and was fairly successful in recovering the residual oil after waterflooding.

3. Permeability and porosity maximum values differed from 30% and 500md (0.5 D) to 48% and 5.5 D (5415md) for field and laboratory criteria respectively. This difference was due to the highly permeable sandpacks used in laboratory experiments. A new method of gravity stable surfactant flooding for horizontal wells with high vertical permeability was tested sucessfully using sandpacks.
4. Maximum residual oil saturation value varied from 58% for field range to 55% for laboratory range. This difference was noted as heavy oil resulted in poor waterflooding recovery and a class of new surfactants was tested for tertiary oil recovery of such heavy oil reservoirs in Canada.
5. Brine salinity and brine hardness maximum values for field were 160,000 and 6,530 ppm. However, for laboratory the values were 350,000 ppm and 36,633. Such high maximum salinity and hardness values were due to the laboratory research carried out to test the stability of surfactants and yield a low IFT value at the same time in highly saline and hard brines.

4.2 CONCLUSION

1. This work gives a detailed description of steps followed to give an updated range for surfactant-polymer flooding on a field and laboratory scale.

2. The field dataset was checked for special cases and inconsistent values for various parameters with the help of histograms and box-plots.
3. Ranges for different imperative laboratory parameters were presented graphically using histograms and box-plots.
4. Eventually, field ranges were compared with the previous work published in the literature and sought for differences.
5. Laboratory and field ranges were compared and their differences were explained.

BIBLIOGRAPHY

1. Enhanced Oil Recovery- Don W. Green & Paul Willhite (1998)

2. E. Manrique et.al., Norwegian University of Science and technology- Chemical flooding projects for enhanced oil recovery (2010)

3. Istvan Lakatos et. al., University of Miskolc, Role of conventional and Unconventional hydrocarbons in the 21st century: comparison of resources, reserves, recovery factors and Technologies. (2009)

4. Department of Energy (DOE), Chemical flooding projects for unconventional hydrocarbons (1993)

5. Schramm L. L., Surfactants fundamental and application in petroleum industry, (2000)

6. Levitt D.B., Identification and evaluation of high-performance EOR surfactant (University of Texas- Austin, 2006)

7. Gary Walker (DOE), Increasing heavy oil reserves in the Willmington oilfield through advanced reservoir characterization and thermal production technologies. (Annual report, March 31, 2000)

8. Alhasan Fuseni (Saudi Aramco), Phase behavior and interfacial tension properties of an amphoteric surfactant for EOR application. (2013)

9. Jean-Louis Salager, Surfactant types and uses. (2002)

10. Xianmin Zhou et. al. Adsorption of an amphoteric surfactant onto permeable carbonate rocks. (2013)

11. Bataweel, M. A., Yadhalli Shivaprasad, A., & Nasr-El-Din, H. A. (2012, January 1). Low-Tension Polymer Flooding Using Amphoteric surfactant in High Salinity/High Hardness and High Temperature Conditions in Sandstone Cores. Society of Petroleum Engineers. doi:10.2118/155676-MS

12. Gao, B., & Sharma, M. M. (2013, June 6). A New Family of Anionic Surfactants for Enhanced-Oil-Recovery Applications. Society of Petroleum Engineers. doi:10.2118/159700-PA

13. Healy, R. N., & Reed, R. L. (1974, October 1). Physicochemical Aspects of Microemulsion Flooding. Society of Petroleum Engineers. doi:10.2118/4583-PA

14. Wade, W. H., Morgan, J. C., Schechter, R. S., Jacobson, J. K., & Salager, J. L. (1978, August 1). Interfacial Tension and Phase Behavior of Surfactant Systems. Society of Petroleum Engineers. doi:10.2118/6844-PA

15. J Salager, J. L., Morgan. C., Schechter, R. S., Wade, W. H., & Vasquez, E. (1979, April 1). Optimum Formulation of Surfactant/Water/Oil Systems for Minimum Interfacial Tension or Phase Behavior. Society of Petroleum Engineers. doi:10.2118/7054-PA

16. Winsor P. A. Binary and Muticomponent solution of amphiphilic compunds. Solubalization and the formation, structure and theoretical significance of liquid crystalline solutions (1967).

17. Thomas, S. (2006, January 1). Chemical EOR: The Past - Does It Have a Future? (Russian). Society of Petroleum Engineers.

18. Salter, S. J. (1977, January 1). The Influence Of Type And Amount Of Alcohol On Surfactant-Oil-Brine Phase Behavior And Properties. Society of Petroleum Engineers. doi:10.2118/6843-MS

19. Li, R. F., Le Bleu, R. B., Liu, S., Hirasaki, G. J., & Miller, C. A. (2008, January 1). Foam Mobility Control for Surfactant EOR. Society of Petroleum Engineers. doi:10.2118/113910-MS

20. Trogus, F. J., Sophany, T., Schechter, R. S., & Wade, W. H. (1977, October 1). Static and Dynamic Adsorption of Anionic and Nonionic Surfactants. Society of Petroleum Engineers. doi:10.2118/6004-PA

21. Schamehorn, J. F., Schechter, R. S., Wade W.H. (1981, April 22). Adsorption of Surfactants on Mineral oxide Surfaces from Aqueous Solutions.

22. Ziegler, V. M., & Handy, L. L. (1981, April 1). Effect of Temperature on Surfactant Adsorption in Porous Media. Society of Petroleum Engineers. doi:10.2118/8264-PA

23. Dang, C. T. Q., Chen, Z. J., Nguyen, N. T. B., Bae, W., & Phung, T. H. (2011, January 1). Development of Isotherm Polymer/Surfactant Adsorption Models in Chemical Flooding. Society of Petroleum Engineers. doi:10.2118/147872-MS

24. Davis, H. T., & Scriven, L. E. (1980, January 1). The Origins Of Low Interfacial Tensions For Enhanced Oil Recovery. Society of Petroleum Engineers. doi:10.2118/9278-MS

25. Cinar, Y., & Orr, F. M. (2004, January 1). Measurement of Three-Phase Relative Permeability with IFT Variation. Society of Petroleum Engineers. doi:10.2118/89419-MS

26. Delshad, M., Delshad, M., Bhuyan, D., Pope, G. A., & Lake, L. W. (1986, January 1). Effect of Capillary Number on the Residual Saturation of a Three-Phase Micellar Solution. Society of Petroleum Engineers. doi:10.2118/14911-MS

27. Bashiri, A., & Kasiri, N. (2011, January 1). Properly Use Effect of Capillary Number on Residual Oil Saturation. Society of Petroleum Engineers. doi:10.2118/150800-MS

28. Sheng, J. J. (2013, April 19). A Comprehensive Review of Alkaline-Surfactant-Polymer (ASP) Flooding. Society of Petroleum Engineers. doi:10.2118/165358-MS

29. Wei, H. (2012, January 1). Molecular Design Synthesis and Simulation on a Novel Gemini Surfactant for EOR From Low Permeability Reservoirs. Society of Petroleum Engineers. doi:10.2118/160854-MS

30. Gogarty, W. B. (1978, August 1). Micellar/Polymer Flooding An Overview. Society of Petroleum Engineers. doi:10.2118/7041-PA

31. Hite, J. R., & Bondor, P. L. (2004, January 1). Planning EOR Projects. Society of Petroleum Engineers. doi:10.2118/92006-MS

32. Manrique, E. J., Thomas, C. P., Ravikiran, R., Izadi Kamouei, M., Lantz, M., Romero, J. L., & Alvarado, V. (2010, January 1). EOR: Current Status and Opportunities. Society of Petroleum Engineers. doi:10.2118/130113-MS

33. Thomas, S., & Ali, S. M. F. (1992, August 1). Micellar-Polymer Flooding: Status And Recent Advances. Petroleum Society of Canada. doi:10.2118/92-08-05

34. Hirasaki, G. J., Miller, C. A., & Puerto, M. (2008, January 1). Recent Advances in Surfactant EOR. Society of Petroleum Engineers. doi:10.2118/115386-MS

35. Brashear, J. P., & Kuuskraa, V. A. (1978, September 1). The Potential and Economics of Enhanced Oil Recovery. Society of Petroleum Engineers. doi:10.2118/6350-PA

36. Carcoana, A. N. (1982, January 1). Enhanced Oil Recovery in Rumania. Society of Petroleum Engineers. doi:10.2118/10699-MS

37. Putz, A., Chevalier, J. P., Stock, G., & Philippot, J. (1981, April 1). A Field Test of Microemulsion Flooding, Chateaurenard Field, France. Society of Petroleum Engineers. doi:10.2118/8198-PA

38. Aguey, O. J. (1982, January 1). Field Performance Analysis of Micellar Polymer Pilot Flood. Society of Petroleum Engineers. doi:10.2118/10732-MS

39. Gupta, S. P. (1984, February 1). Compositional Effects on Displacement Mechanisms of the Micellar Fluid Injected in the Sloss Field Test. Society of Petroleum Engineers. doi:10.2118/8827-PA

40. Staub, H. L. (1981, January 1). Results Of A Micellar-Polymer Flood In A Flooded-Out, Low Gravity Reservoir. Society of Petroleum Engineers. doi:10.2118/9791-MS

41. Aho, G. E., & Bush, J. (1982, January 1). Results of the Bell Creek Unit 'A' Micellar-Polymer Pilot. Society of Petroleum Engineers. doi:10.2118/11195-MS

42. Hamaker, D. E., & Frazier, G. D. (1978, January 1). Manvel Enhanced Recovery Pilot Design And Implementation. Society of Petroleum Engineers. doi:10.2118/7088-MS

43. Cooper, M. N., Southworth, R. A., Walsh, D. M., & Morgan, J. C. (1985, January 1). Field Experience In The Bothamsall Surfactant Flood Project. Society of Petroleum Engineers. doi:10.2118/13990-MS

44. Luo, P., Wu, Y., & Huang, S.-S. S. (2013, June 11). Optimized Surfactant-Polymer Flooding for Western Canadian Heavy Oils. Society of Petroleum Engineers. doi:10.2118/165396-MS

45. Lu, J., Britton, C., Solairaj, S., Liyanage, P. J., Kim, D. H., Adkins, S., … Pope, G. A. (2012, January 1). Novel Large-Hydrophobe Alkoxy Carboxylate Surfactants for Enhanced Oil Recovery. Society of Petroleum Engineers. doi:10.2118/154261-MS

46. Ziegler, V. M. (1988, May 1). Laboratory Investigation of High Temperature Surfactant Flooding. Society of Petroleum Engineers. doi:10.2118/13071-PA

47. Morvan, M., Degre, G., Beaumont, J., Dupuis, G., Zaitoun, A., Al-maamari Rashid Salim, … Al-Sharji, H. H. (2012, January 1). Optimization of Viscosifying Surfactant Technology for Chemical EOR. Society of Petroleum Engineers. doi:10.2118/154053-MS

48. Bae, J. H., & Petrick, C. B. (1986, November 1). Glenn Pool Surfactant Flood Pilot Test: Comparison of Laboratory and Observation-Well Data. Society of Petroleum Engineers. doi:10.2118/12694-PA

49. Murtada, H., & Marx, C. (1982, December 1). Evaluation of the Low Tension Flood Process for High-Salinity Reservoirs-Laboratory Investigation Under Reservoir Conditions. Society of Petroleum Engineers. doi:10.2118/8999-PA

50. Pope, G. A., Weerasooriya, U. P., & Lu, J. (2013, April 8). Stability Investigation in Low-Tension Surfactant Floods. Society of Petroleum Engineers. doi:10.2118/164090-MS

51. Sarma, H. K., Maini, B. B., & Jha, K. (1998, July 1). Evaluation of Emulsified Solvent Flooding For Heavy Oil Recovery. Petroleum Society of Canada. doi:10.2118/98-07-06

52. Stournas, S. (1983, January 1). Brine-Resistant Sulfonate Surfactants for Enhanced Oil Recovery. Society of Petroleum Engineers. doi:10.2118/11773-MS

53. Lu, J., Weerasooriya, U. P., Solairaj, S., Kim, D. H., Liyanage, P. J., Pope, G. A., … Britton, C. (2013, March 26). Recent Technology Developments in Surfactants and Polymers for Enhanced Oil Recovery. International Petroleum Technology Conference. doi:10.2523/16425-MS

54. Nguyen, P.-T., Do, B.-P. H., Pham, D.-K., Nguyen, Q.-T., Dao, D.-Q. P., & Nguyen, H.-A. (2012, January 1). Evaluation on the EOR Potential Capacity of the Synthesized Composite Silica-Core/ Polymer-Shell Nanoparticles Blended with Surfactant Systems for the HPHT Offshore Reservoir Conditions. Society of Petroleum Engineers. doi:10.2118/157127-MS

55. Ibrahim, Z. B., Manap, A. A. A., Hamid, P. A., Hon, V. Y., Lim, P. H., & Wyatt, K. (2006, January 1). Laboratory Aspect of Chemical EOR Processes Evaluation for Malaysian Oilfields. Society of Petroleum Engineers. doi:10.2118/100943-MS

56. Bouabboune, M., Hammouch, N., & Benhadid, S. (2006, January 1). Comparison Between Micro-Emulsion and Surfactant Solution Flooding Efficiency for Enhanced Oil Recovery in TinFouye Oil Field. Petroleum Society of Canada. doi:10.2118/2006-058

57. Maudgalya, S., Knapp, R. M., McInerney, M. J., Folmsbee, M., & Nagle, D. P. (2005, January 1). Tertiary Oil Recovery With Microbial Biosurfactant Treatment of Low-Permeability Berea Sandstone Cores. Society of Petroleum Engineers. doi:10.2118/94213-MS

58. Michels, A. M., Djojosoeparto, R. S., Haas, H., Mattern, R. B., van der Weg, P. B., & Schulte, W. M. (1996, August 1). Enhanced Waterflooding Design With Dilute Surfactant Concentrations for North Sea Conditions. Society of Petroleum Engineers. doi:10.2118/35372-PA

59. Najurieta, H. L., Galacho, N., Chimienti, M. E., & Illiano, S. N. (2001, January 1). Effects of Temperature and Interfacial Tension in Different Production Mechanisms. Society of Petroleum Engineers. doi:10.2118/69398-MS

60. Tabary, R., Douarche, F., Bazin, B., Lemouzy, P. M., Moreau, P., & Morvan, M. (2012, January 1). Design of a Surfactant/Polymer Process in a Hard Brine Context: A Case Study Applied to Bramberge Reservoir. Society of Petroleum Engineers. doi:10.2118/155106-MS

61. Hill, H. J., Reisberg, J., 10& Stegemeier, G. L. (1973, February 1). Aqueous Surfactant Systems For Oil Recovery. Society of Petroleum Engineers. doi:.2118/3798-PA

62. Wasan, D. T., Shah, S. M., Aderangi, N., Chan, M. S., & McNamara, J. J. (1978, December 1). Observations on the Coalescence Behavior of Oil Droplets and Emulsion Stability in Enhanced Oil Recovery. Society of Petroleum Engineers. doi:10.2118/6846-PA

63. Al-Adasani, A., & Bai, B. (2010, January 1). Recent Developments and Updated Screening Criteria of Enhanced Oil Recovery Techniques. Society of Petroleum Engineers. doi:10.2118/130726-MS

VITA

Pratap Chauhan earned his under graduate degree (B.Sc.) in Geology from University of Pune, Maharashtra, India in spring 2009. He earned a master's degree in Petroleum Technology (M.Sc) from University of Pune in the spring of 2011. In August, 2014, he received his Master in Petroleum Engineering degree from Missouri University of Science and Technology.